Large liquid detectors in Europe: Scientific Case

J. Äystö,[1] A. Badertscher,[2] L. Bezrukov,[3] J. Bouchez,[4] A. Bueno,[5] J. Busto,[6] J.-E. Campagne,[7] Ch. Cavata,[8] A. de Bellefon,[9] J. Dumarchez,[10] J. Ebert,[11] T. Enqvist,[12] A. Ereditato,[13] F. von Feilitzsch,[14] M. Göger-Neff,[14] S. Gninenko,[15] W. Gruber,[2] C. Hagner,[11] K. Hochmuth,[16] J. Holeczek,[17] J. Kisiel,[17] L. Knecht,[2] I. Kreslo,[13] V. A. Kudryavtsev,[18] P. Kuusiniemi,[12] T. Lachenmaier,[15] M. Laffranchi,[2] B. Lefievre,[9] M. Lindner,[19] J. Maalampi,[20] A. Marchionni,[2] T. Marrodán Undagoitia,[14] A. Meregaglia,[2] M. Messina,[13] M. Mezzetto,[21] L. Mosca,[15] U. Moser,[13] A. Müller,[2] G. Natterer,[2] L. Oberauer,[14] P. Otiougova,[2] T. Patzak,[9] J. Peltoniemi,[12] W. Potzel,[14] C. Pistillo,[13] G. G. Raffelt,[16] M. Roos,[22] B. Rossi,[13] A. Rubbia,[2] N. Savvinov,[13] N. Spooner,[18] A. Tonazzo,[9] W. Trzaska,[1] J. Ulbricht,[2] C. Volpe,[23] J. Winter,[14] M. Wurm,[14] A. Zalewska,[15] and R. Zimmermann[11]
(LAGUNA collaboration)[*]
P. Fileviez Perez,[24] A. Mirizzi,[25] and T. Schwetz[26]
[1] *Department of Physics, University of Jyväskylä, Finland*
[2] *Institut für Teilchenphysik, ETHZ, CH-8093 Zürich, Switzerland*
[3] *Institute for Nuclear Research, Russian Academy of Sciences, Moscow, 117312 Russia*
[4] *CEA - Saclay, 91191 Gif sur Yvette Cedex and APC Paris, France*
[5] *Dpto Fisica Teorica y del Cosmos & C.A.F.P.E., Universidad de Granada, Spain*
[6] *Centre de Physique des Particules de Marseille (CPPM), IN2P3-CBRS et Université d'Aix-Marseille II, 163 Av. de Luminy, B.P. 902, 13288 Marseille Cedex 09, France*
[7] *Laboratoire de l'Accélérateur Linéaire (LAL), IN2P3-CNRS et Université PARIS-SUD 11, Centre Scientifique d'Orsay, B.P. 34, 91898 ORSAY Cedex, France*
[8] *CEA - Saclay, 91191 Gif sur Yvette Cedex, France*
[9] *Astroparticule et Cosmologie (APC), UMR 7164 (CNRS, Universiti Paris VII, CEA, Observatoire de Paris), 11 pl. Marcelin Berthelot, 75231 Paris Cedex 05, France*
[10] *Laboratoire de Physique Nucléaire et des Hautes Energies (LPNHE), IN2P3-CNRS et Universités Paris VI et Paris VII, 4 place Jussieu, Tr. 33 - RdC, 75252 Paris Cedex 05, France*
[11] *Universität Hamburg, Institut für Experimentalphysik, Geb. 67/216, Luruper Chaussee 149, 22761 Hamburg, Germany*
[12] *CUPP, University of Oulu, Finland*
[13] *Laboratory for High Energy Physics, University of Bern, Sidlerstrasse, 5, CH-3012 Bern, Switzerland*
[14] *Technische Universität München, Physik-department E15, James-Franck-Str., 85748 Garching, Germany*
[15] *Unknown*
[16] *Max-Planck-Institut für Physik (Werner-Heisenberg-Institut), Föhringer Ring 6, 80805 München, Germany*
[17] *Institute of Physics, University of Silesia, Uniwersytecka 4, PL-40007 Katowice, Poland*
[18] *Particle Physics and Particle Astrophysics, Department of Physics and Astronomy, University of Sheffield, Hicks Building, Hounsfield Road, Sheffield S3 7RH, UK*
[19] *Max-Planck-Institut fuer Kernphysik, Saupfercheckweg 1, D-69117 Heidelberg, Germany*
[20] *University of Jyväskylä, Finland*
[21] *INFN-Univ. di Padova, Dept. di Fisica, via Marzolo 8, 35100 Padua, Italy*
[22] *Department of Physical Sciences, University of Helsinki, Finland*
[23] *Institut de Physique Nucleaire d'Orsay (IPNO), Groupe de Physique Theorique, Universite de Paris-Sud XI, Bat 100, rue Georges Clemenceau, 91406 Orsay, Cedex, France*
[24] *Centro de Fisica Teorica de Particulas, Instituto Superior Tecnico, Departamento de Fisica, Av. Rovisco Pais 1, 1049-001 Lisboa, Portugal*
[25] *Università di Bari, Dipartimento di Fisica, Via Amendola 173, 70126 Bari, Italy*
[26] *CERN, Physics Department, Theory Division, 1211 Geneva 23, Switzerland*

(Dated: February 27, 2007)

This document contains a comprehensive study of the non-accelerator and accelerator physics potential of three future large-scale detectors proposed in Europe: MEMPHYS (Water Čerenkov), GLACIER (Liquid Argon TPC) and LENA (Liquid Scintillator).

Contents

[*]Electronic address: hep-project-laguna@cern.ch

I. PHYSICS MOTIVATION

The decay of proton is the most exciting prediction of Grand Unified Theories (Nath and Perez, 2006). Several experiments have been built to search for it, with no discovery yet. The window between predicted (in the simplest models typically below 10^{37} years) and excluded (Kobayashi *et al.*, 2005) (O(10^{33}) years, depending on the channel) lifetimes is, however, within our reach, and the demand to fill the gap grows. Also a negative result would be important to rule out certain models (like minimal SU(5) (Georgi and Glashow, 1974)) or constrain the parameter range. Identifying the proton decay and life time would set a firm scale for any unified theory, narrowing the scope for possible models and their parameters. This would be a mandatory step to go forward with the physics beyond the Standard Model, now partially stalled due to missing experimental data.

The interior of the Earth is known unbelievably ill. We know much better what happens inside the Sun than inside our own planet. There are very few messengers that can give information from below the reach of drill holes, and mere theory is not sufficient for building a credible model for the Earth. However, there is a new unexploited window to the Earth interior, by observing neutrinos produced in the radioactive decays of heavy elements in the matter. Until now only KamLAND experiment (Araki *et al.*, 2005a) has been able to study geoneutrinos, but its event rate does not allow significant conclusions.

Neutrinos are important messengers from stars. Indeed, neutrino astronomy has a glorious history, from the detection of solar neutrinos (Abdurashitov *et al.*, 1994; Aharmim *et al.*, 2005; Altmann *et al.*, 2005; Anselmann *et al.*, 1992; Davis *et al.*, 1968; Hirata *et al.*, 1989; Smy, 2003) to the observation of neutrinos from a supernova (Alekseev *et al.*, 1988; Bionta *et al.*, 1987; Hirata *et al.*, 1987), acknowledged by Nobel Prizes for Koshiba and Ray Davis. These observations have given valuable information both from the stars and from the properties of the neutrinos. However, much more information would be available, if the neutrino spectra of stellar neutrinos would be known better. While the properties of neutrinos become better defined by other experiments, specific neutrino observations could give detailed information on the conditions of the production zone, whether in the Sun or a future galactic supernova. The latter would be extremely important as the explosion of the collapsed star is still a puzzle. An even more fascinating challenge would be to observe neutrinos from extragalactic supernovae, either from identified sources or a diffuse flux from unidentified supernovae from the past.

Observing neutrinos produced in the atmosphere as cosmic ray secondaries (Aglietta *et al.*, 1989; Allison *et al.*, 1999; Ashie *et al.*, 2005; Becker-Szendy *et al.*, 1992; Daum *et al.*, 1995; Hirata *et al.*, 1988a, 1992) gave the first compelling evidence on neutrino oscillation (Fukuda *et al.*, 1998). While the puzzle of missing atmospheric neutrinos can be considered solved, there remains challenges to study the sub dominant oscillation phenomena. Particularly, precise measurements of atmospheric neutrinos would help to resolve ambiguities and degeneracies that hamper the interpretation of other experiments, particularly future long baseline neutrino oscillation searches.

These fascinating phenomena can be investigated with novel multipurpose experiments. The new experiments must be necessarily very large and they must have extremely low background. The required signal to noise ratio can be achieved only in well protected laboratories deep underground. We identify three complementary technologies to respond to the challenge:

1. Water Čerenkov detector: As the cheapest available target material water is the only liquid that is realistic for extremely large detectors, up to several hundreds or thousands of kilotons. Water Čerenkov detectors have rather good resolution for energy, position and direction. The technology is well proven, used previously in IMB, Kamiokande and SuperKamiokande.

2. Liquid Scintillator: Experiments using liquid scintillators provide a high energy resolution and a low energy threshold. They are particularly attractive for low energy detection, for example solar neu-

trinos or geoneutrinos. Liquid scintillator detectors are also based on an established technology, to name Borexino (Back *et al.*, 2004) and KamLAND (Araki *et al.*, 2005b) as examples of previous experiments of regular scale.

3. Liquid Argon: Cryogenic Time Projection Chambers have very good resolution to identify particles. Liquid Argon detectors are very versatile and work well with wide energy range. Experience from such detectors has been gained with ICARUS (Amerio *et al.*, 2004; Arneodo *et al.*, 2001).

Three experiments are proposed to employ these techniques: MEMPHYS (de Bellefon *et al.*, 2006) for Water Čerenkov, LENA (Marrodán Undagoitia *et al.*, 2006; Oberauer *et al.*, 2005) for Liquid Scintillator and GLACIER (Ereditato and Rubbia, 2005; Rubbia, 2004a,b) for Liquid Argon. The purpose of this report is to study the physics potential of these experiments and rise some complementary aspects between the three techniques.

Possible neutrino beams from future accelerators would provide an additional bonus for these experiments. Measuring the oscillation of controllably made neutrinos with a sufficiently long baseline would allow to determine the properties of neutrinos (particularly the mixing angle θ_{13}, as well as CP violation) with an improved accuracy. The considered detectors may be used for observing neutrinos from beta and superbeams, in the optimal energy range characteristic to each experiment. A common example is a low energy ($\gamma \sim 100$) beta beam from CERN to MEMPHYS at Frejus, 130 km apart (Campagne *et al.*, 2006). However, higher energy beams up to O(6 GeV) have been suggested (Rubbia *et al.*, 2006), favouring longer distances up to O(2000 km). The neutrino factory would require a magnetized detector, which is beyond the scope of this study.

A major experiment provides possibilities for major surprises. The history of neutrino astrophysics, like the history of science, has demonstrated that many experiments have made their glory with other discoveries that they were mainly intended for, just to name the proton decay experiments observing neutrinos. All of the three proposed experiments, with a huge improvement on size and resolution, will have a significant potential for surprises to be discovered.

II. BRIEF DETECTOR DESCRIPTION

The three detectors basic parameters are listed in Tab. I. All of them have active targets of tens to hundreds kilotons in mass and are situated in underground laboratories to be protected against background induced by cosmic rays. The large size of these detectors is motivated by the extremely low cross sections of neutrinos and/or the rareness of the interesting events searched for.

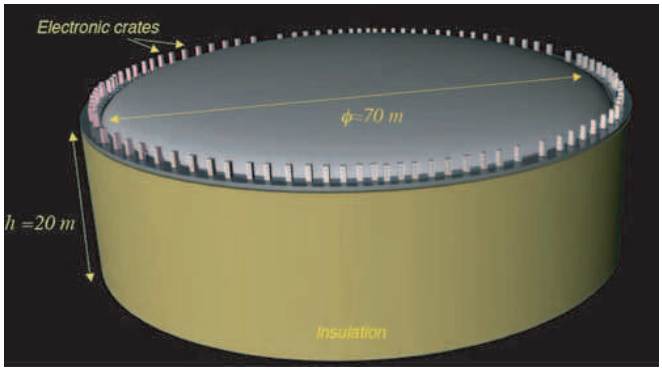

FIG. 1 An artistic view of a 100 kton single tanker liquid argon detector. The electronic crates are located at the top of the dewar.

Some details of the detectors are discussed in the following sections while the Underground site related matter is discussed in section III.

A. Liquid Argon TPC

GLACIER (Fig. 1) is the foreseen extrapolation up to 100 kT of a Liquid Argon Time Projection Chamber.

The detector can be mechanically subdivided into two parts: (1) the liquid argon tanker and (2) the inner detector instrumentation. For simplicity, we assume at this stage that the two aspects can be decoupled.

The basic idea behind this detector is to use a single 100 kton "boiling" cryogenic tanker with Argon refrigeration (in particular, the cooling is done directly with Argon, e.g. without nitrogen). Events can be reconstructed in 3D using the information provided by ionization, in the fact the imaging capabilities make this detector an "electronic bubble chamber". Scintillation and Čerenkov light readout complete the event information.

One can profit from the ICARUS R&D which has shown that it is possible to operate PMTs immersed directly in the liquid Argon (Amerio *et al.*, 2004). In order to be sensitive to DUV scintillation, the PMTs are coated with a wavelength shifter (Tetraphenyl-Butadiene). About 1000 immersed phototubes with WLS would be used to identify the (isotropic and bright) scintillation light. To detect Čerenkov radiation about 27000 immersed 8"-phototubes without WLS would provide a 20% coverage of the surface of the detector. As already mentioned, these latter PMTs should have single photon counting capabilities in order to count the number of Čerenkov photons.

Charge amplification and an extreme purity is needed to allow the foreseen long drifts (≈ 20 m), so the detector will run in bi-phase mode. Namely, drift electrons produced in the liquid phase are extracted from the liquid into the gas phase with the help of an electric field of the order of 3 kV/cm to compensate the charge attenuation along drift. The charge will be amplied and read

TABLE I Some basic parameters of the three detector baseline designs. The underground laboratory related matter are described in section III

	GLACIER	LENA	MEMPHYS
Detector dimensions			
type	vertical cylinder	horizontal cylinder	$3 \div 5$ shafts
diam. x length	$\phi = 70\text{m} \times L = 20\text{m}$	$\phi = 30\text{m} \times L = 100\text{m}$	$(3 \div 5) \times (\phi = 65\text{m} \times H = 65\text{m})$
typical mass (kt)	100	50	$440 \div 730$
Active target and readout[†]			
type of target	liquid argon (boiling)	liquid scintillator	water (option: 0.2% $GdCl_3$)
readout type			
e^- drift	2 perp. views, 10^5 channels, ampli. in gas phase	12,000 20" PMTs $\gtrsim$ 30% coverage	81,000 12" PMTs $\sim$ 30% coverage
Č light	27,000 8" PMTs, $\sim$ 20% coverage		
Scint. light	1,000 8" PMTs		

by means of Large Electron Multiplier (LEM) devices. A possible extension of the present design is the use of an external magnetic field.

Contact with the LNG (Liquefied Natural Gas) and Technodyne LtD have been taken to make feasibility studies to build such cryogenic detector in underground site.

B. Liquid Scintillator

The LENA detector is cylindrical in shape, with a length of about 100 m and 30 m diameter (Fig. 2). An inside part of 13 m radius contains approximately 5×10^7 m^3 of liquid scintillator while the outside part is filled with water acting as a muon veto. Both the outer and the inner volume are enclosed in steel tanks of 3 to 4 cm wall thickness. For most purposes, a fiducial volume at 1 m distance to the inner tank walls is defined, corresponding to 88 % of the inner detector volume.

The axis of the detector is aligned horizontally. A tunnel-shaped cavern harbouring the detector is well feasible at most locations. In respect to accelerator physics, the axis should be oriented towards the neutrino source (e.g. CERN) in order to contain the full length of muon and electron tracks.

The default setting for light detection in the inner detector is the mounting of 12 000 photomultipliers (PMTs) of 20" diameter each to the inner cylinder wall, covering about 30 % of the surface. As an option, light concentrators can be installed in front of the PMTs, increasing the surface coverage c to values of more than 50 %. Alternatively, $c = 30\,\%$ can be reached by the equipment of 8" PMTs with light concentrators, thereby reducing costs compared to the default setting. Additional PMTs are

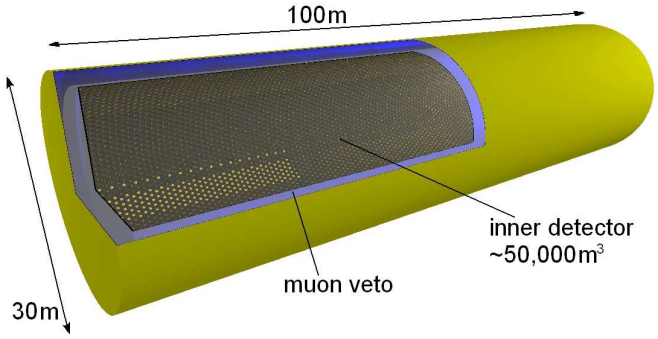

FIG. 2 Sketch of the LENA detector.

supplied in the outer muon veto to detect the Čerenkov light of incoming particles.

Possible candidates for the liquid scintillator are (1.) pure PXE (phenyl-o-xylylethane), (2.) a mixture of 20 % PXE and 80 % Dodecane, or (3.) Linear Alkylbenzene (LAB). All three liquids are of minor toxicity to the environment and provide high flash and inflammation points.

C. Water Čerenkov

The MEMPHYS detector (Fig. 3) is an extrapolation of SuperKamiokande up to 730 kT. This Water Čerenkov detector is a collection of up to 5 shafts, and 3 are enough for 440 kt fiducial mass which is used hereafter. Each shaft is 65 m in diameter and 65 m height for the total water container dimensions, and this represent an extrapolation of a factor 4 with respect to the Super-Kamiokande running detector. The PMT surface defined as 2 m inside the water container is covered by about 81,000 12" PMTs to reach a 30% surface coverage equivalent to a

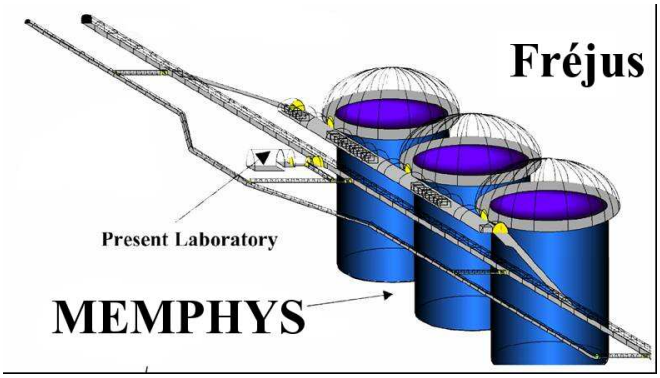

FIG. 3 Sketch of the MEMPHYS detector under the Fréjus mountain (Europe).

40% coverage with 20" PMTs. The fiducial volume is defined by an additional conservative guard of 2 m. The outer volume between the PMT surface and the water vessel is instrumented with 8" PMTs. If not contrary mentionned, the Super-Kamiokande analysis (efficiency, background reduction) is used to compute the physcis potential of such a detector. In the US and in Japan, there are two competitors to MEMPHYS, namely UNO and Hyper-Kamiokande. These projects are similar in many respects and the hereafter presented physics potential may be transposed also for those detectors[1]. Currently, there is a very promising on going R&D activity concerning the possibility to introduce Gadolinium salt ($GdCl_3$) in side SuperKamiokande. The physics goal is to decrease the background in many physics channels by tagging the neutron produced in the inverse beta decay interaction of $\bar{\nu}_e$ on free protons. For instance, 100 tons of $GdCl_3$ in Super-Kamiokande would yield more then 90% neutron captures on Gd (Beacom and Vagins, 2004).

III. UNDERGROUND SITES

The proposed large detectors require underground laboratories of adequate size and depth, naturally protected against cosmic rays, which represent a potential source of background events mainly for non-accelerator experiments. Additional characteristics of these sites contributing to qualify them as best candidates for the proposed projects of experiments are: the type and quality of the rock allowing the feasibility of such a large caverns at reasonable cost and time, the distance from existing or future accelerators and nuclear reactors, the type and quality of the access, the geographical position, the quality of the environment, etc.

The presently pre-selected candidate sites in the world are essentially located in 3 regions : North-America, Asia (Japan/Korea, ...) and Europe. In this paper we consider the European region, where, at this stage, the following sites are assumed as candidates: Gran Sasso (Italy), Fréjus (France/Italy), Pyhäsalmi (Finland), Boulby (UK), Canfranc (Spain) and Sieroszewice (Poland). The basic characteristics of these sites are presented on Tab. II. For the Gran Sasso case, possible new sites are envisaged to be located at 10km from the present underground laboratory outside the National Park. The possibility of under-water solutions, as for instance Pylos for the LENA project, is not taken into account here.

The identification and measurement of the different background components in the candidate sites (muons, fast neutrons from muon interactions, slow neutrons from nuclear reactions in the rock, gammas, electrons/positrons and alphas from radioactive decays,...) is underway mainly in the context of the ILIAS European (JRA) Network. The collection of the presently known values of these background components are reported on Tab. II.

None of the existing sites have yet a cavity to accommodate the foreseen detectors. For two of the candidate sites (Fréjus and Pyhäsalmi), a preliminary feasibility study for large excavation at a deep depth has been already performed. For the Fréjus site the main conclusion from the simulations (in 2005) constrained by a series of rock parameters measurements made during the Fréjus road tunnel excavation, is that the "shaft shape" is strongly preferred compared to the "tunnel shape" for large cavities. Several (up to 5) such shafts cavities with a diameter of about 65 m (a volume of 250 000 m^3) each, seem feasible in the region around the middle of the Fréjus tunnel, at a depth of 4800 m.w.e, where by chance the quality of the rock is the best. For the Pyhäsalmi site the preliminary study has been performed (in 2002) for two main cavities with tunnel-shape and dimensions $(20 \times 20 \times 120)$ m^3 and $(20 \times 20 \times 50)$ m^3 respectively, and one shaft-shaped cavity with 25 m in diameter and 25 m in height, all at a depth of about 1430 m of rock (4000 m.w.e).

IV. PROTON DECAY SENSITIVITY

For all relevant aspects of the proton stability in grand unified theories, in strings and in branes see reference (Nath and Perez, 2006).

Since proton decay is the most dramatic prediction coming from theories where the matter is unified, we hope to test those scenarios at future experiments. For this reason, a theoretical upper bound on the lifetime of the proton is very important to know about the possibilities of future experiments.

Recently a model-independent upper bound on the total proton decay lifetime has been pointed out (Dorsner and Perez, 2005a):

TABLE II Summary of relevant characteristics of some sites foreseen for the proposed detectors. The Rn content depends on the ventilation of the cavity. The "*" means that the parameter is not yet available. To be completed and cross-checked and unit uniformized as possible.

Site	Gran Sasso ext.	Fréjus	Pyhäsalmi	Boulby	Canfranc	Sieroszowice
Location	Italy	Italy-France border	Finland	UK	Spain	Poland
Distance from CERN (km)	730	130	2300	1050	630	950
Type of access	?	Fréjus tunnel	Mine	Potash Mine	Somport tunnel	Mine
Vertical Depth (m.w.e)	?	4800	4000	3300	2500	2200
Type of rock	hard rock	hard rock	hard rock	salt	hard rock	salt & rock
Type/size of cavity	?	shafts $\Phi = 65$ m, $H = 80$ m	tunnel 20 m × 20 m × 120 m	?	*	tunnel 15 m × 15 m × 100 m
μ Flux (10^{-9} cm^{-2}s^{-1})	?	4.8	?	41.7	200.0	?
n Flux (10^{-6} cm^{-2}s^{-1})	?	1.6 (0-0.63 eV) 4.0 (2-6 MeV)	?	2.8 (>100 keV) 1.3 (>1 MeV)	3.82 (integral)	*
γ Flux (cm^{-2}s^{-1})	?	7.0 (>4 MeV)	*	*	2 10^{-2} (energy?)	*
^{238}U (ppm) Rock/Cavern	?	0.84/1.90	28-44 Bq/m^3	0.07	30 Bq/kg	0.017 ± 0.003 Bq/kg
^{232}Th (ppm) Rock/Cavern	?	2.45/1.40	4-19 Bq/m^3	0.12	76 Bq/kg	0.008 ± 0.001 Bq/kg
K (Bq/kg) Rock/Cavern	?	213/77	267-625 Bq/m^3	1130	680	4.0 ± 0.9 Bq/kg
Rn (Bq/m^3) Cavern (Vent. ON/OFF)	?	15-150	10-148	*	50-100 Bq/kg	$10 - 50$

$$\tau_p^{upper} = \left\{ \begin{array}{ll} 6.0 \times 10^{39} & \text{(Majorana case)} \\ 2.8 \times 10^{37} & \text{(Dirac case)} \end{array} \right\} \times \frac{\left(M_X/10^{16} GeV\right)^4}{\alpha_{GUT}^2} \times \left(\frac{0.003 GeV^3}{\alpha}\right)^2 \text{ yrs} \quad (1)$$

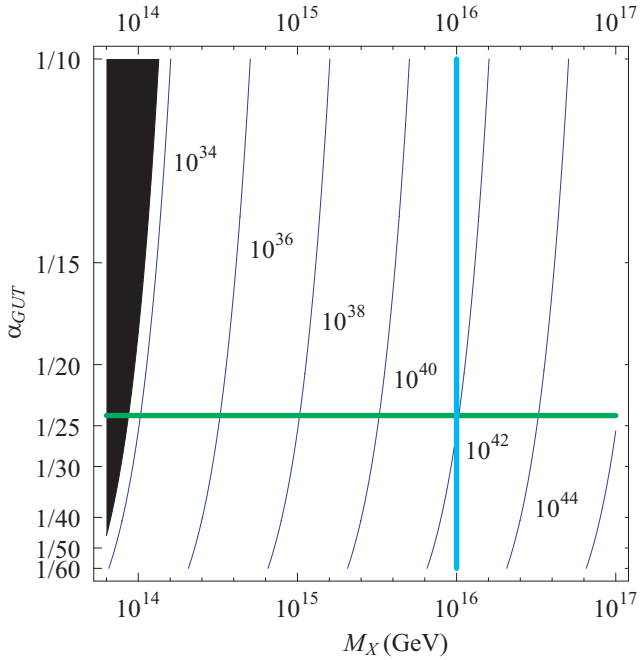

FIG. 4 Isoplot for the upper bounds on the total proton lifetime in years in the Majorana neutrino case in the M_X–α_{GUT} plane. The value of the unifying coupling constant is varied from 1/60 to 1/10. The conventional values for M_X and α_{GUT} in SUSY GUTs are marked in thick lines. Experimentally excluded region is given in black (Dorsner and Perez, 2005a).

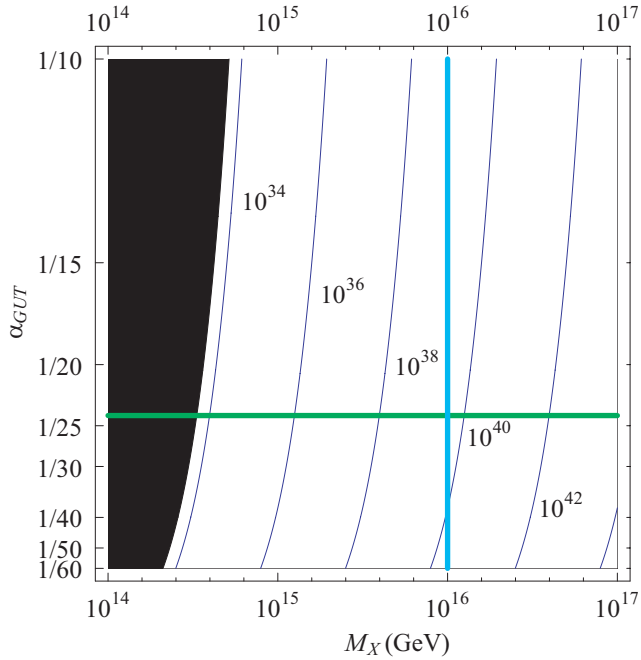

FIG. 5 Isoplot for the upper bounds on the total proton lifetime in years in the Dirac neutrino case in the M_X–α_{GUT} plane. The value of the unifying coupling constant is varied from 1/60 to 1/10. The conventional values for M_X and α_{GUT} in SUSY GUTs are marked in thick lines. Experimentally excluded region is given in black (Dorsner and Perez, 2005a).

where M_X is the mass of the superheavy gauge bosons. The parameter $\alpha_{GUT} = g_{GUT}^2/4\pi$, where g_{GUT} is the gauge coupling at the grand unified scale. α is the matrix element. See Fig. 4 and Fig. 5 for the present parameter space allowed by the experiments.

Most of the models (Supersymmetric or non-Supersymmetric) predict a lifetime τ_p below those upper bounds 10^{33-37} years, which are very interesting since it is the possible range of the proposed detectors.

In order to have an idea of the proton decay predictions, let us list in Tab. III the results in different models.

No specific simulation for MEMPHYS has been carried out yet. We therefore rely on the study done by UNO, adapting the results to MEMPHYS (which has an overall better coverage) when possible.

To study the physics potentialities of very large underground Liquid Argon Time Projection Chambers (LAr TPC), a detailed simulation of signal efficiency and background sources, including atmospheric neutrinos and cosmogenic backgrounds was carried out (Bueno *et al.*, 2007). Liquid Argon TPCs, offering good granularity and energy resolution, low particle detection threshold, and excellent background discrimination, should yield very good signal over background ratios in many possible decay modes, allowing to reach partial lifetime sensitivities in the range of $10^{34} - 10^{35}$ years with exposures up to 1000 kton×year, often in quasi-background-free conditions optimal for discoveries at the few events level, corresponding to atmospheric neutrino background rejections of the order of 10^5. Multi-prong decay modes like e.g. $p \to \mu^- \pi^+ K^+$ or $p \to e^+ \pi^+ \pi^-$ and channels involving kaons like e.g. $p \to K^+ \bar{\nu}$, $p \to e^+ K^0$ and $p \to \mu^+ K^0$ are particularly suitable, since liquid Argon imaging provides typically an order of magnitude improvement in efficiencies for similar or better background conditions compared to Water Cerenkov detectors. Up to a factor 2 improvement in efficiency is expected for modes like $p \to e^+ \gamma$ and $p \to \mu^+ \gamma$ thanks to the clean photon identification and separation from π^0. Channels like $p \to e^+ \pi^0$ or $p \to \mu^+ \pi^0$, dominated by intrinsic nuclear

TABLE III Summary of some recent predictions on proton partial lifetimes. Some references for the different models are: (1) (Georgi and Glashow, 1974), (2) (Dorsner and Perez, 2005b; Dorsner *et al.*, 2006), (3) (Lee *et al.*, 1995), (4) (Bajc *et al.*, 2002a,b; Emmanuel-Costa and Wiesenfeldt, 2003; Murayama and Pierce, 2002), (5) (Aulakh *et al.*, 2004; Babu and Mohapatra, 1993; Fukuyama *et al.*, 2004; Goh *et al.*, 2004), (6) (Friedmann and Witten, 2003)

Model	Decay modes	Prediction	References
Georgi-Glashow model	-	ruled out	(1)
Minimal realistic non-SUSY $SU(5)$	all channels	$\tau_p^{upper} = 1.4 \times 10^{36}$	(2)
Two Step Non-SUSY SO(10)	$p \to e^+\pi^0$	$\approx 10^{33-38}$	(3)
Minimal SUSY $SU(5)$	$p \to \bar{\nu}K^+$	$\approx 10^{32-34}$	(4)
SUSY $SO(10)$ with 10_H, and 126_H	$p \to \bar{\nu}K^+$	$\approx 10^{33-36}$	(5)
M-Theory(G_2)	$p \to e^+\pi^0$	$\approx 10^{33-37}$	(6)

effects, yield similar efficiencies and backgrounds as in Water Cerenkov detectors. An extremely important feature of GLACIER is that thanks to the self-shielding and 3D-imaging properties of the liquid Argon TPC, this result remains valid even at shallow depths where cosmogenic background sources are important. The possibility of a very large area annular active muon veto shield in order to further suppress cosmogenic backgrounds at shallow depths is also a very promising option to complement the GLACIER detector.

In order to quantitatively estimate the potential of the LENA detector for measuring the proton lifetime, a Monte Carlo simulation for the decay channel $p \to K^+\overline{\nu}$ has been performed. For this purpose, the Geant4 simulation toolkit has been used (Agostinelli *et al.*, 2003). Not only all default Geant4 physics lists were included but also optical processes as scintillation, Cherenkov light production, Rayleigh scattering and light absorption. From these simulations a light yield of ~ 110 pe/MeV for an event in the center of the detector results. In addition, to take into account the so called quenching effects, the semi-empirical Birk's formula (Birks, 1964) has been introduced into the code.

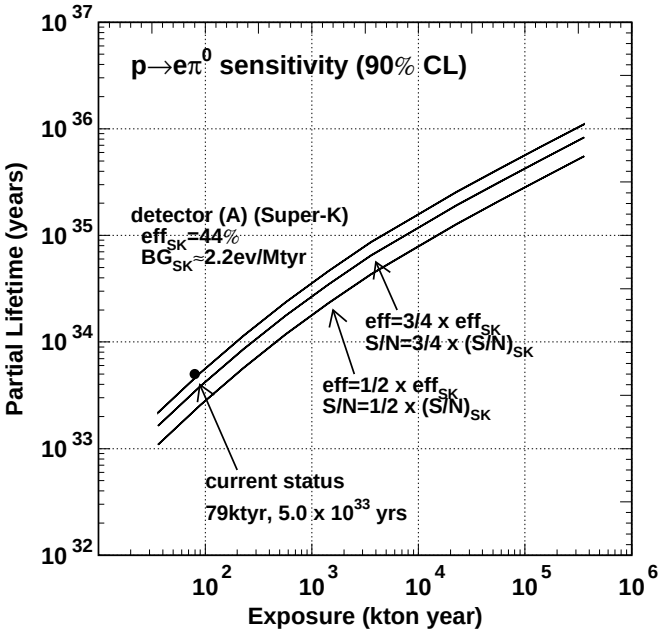

FIG. 6 Sensitivity for $e^+\pi^0$ proton decay lifetime, as determined by UNO (Jung, 2000). MEMPHYS corresponds to case (A).

A. $p \to e^+\pi^0$

Following UNO study, the detection efficiency of $p \to e^+\pi^0$ (3 showering rings event) is $\epsilon = 43\%$ for a 20 inch-PMT coverage of 40% or its equivalent, as envisioned for MEMPHYS. The corresponding estimated atmospheric neutrino induced background is at the level of 2.25 events/Mt.yr. From these efficiencies and background levels, proton decay sensitivity as a function of detector exposure can be estimated. A 10^{35} years partial lifetime (τ_p/B) could be reached at the 90% C.L. for a 5 Mt.yr exposure (10 yrs) with MEMPHYS (similar to case A in Fig. 6). Beyond that exposure, tighter cuts may be envisaged to further reduce the atmospheric neutrino background to 0.15 events/Mt.yr, by selecting quasi exclusively the free proton decays.

The positron and the two photons issued from the π^0 gives clear events in the GLACIER detector. We find that the π^0 is absorbed by the nucleus $\sim$45% of the times. Assuming a perfect particle and track identification, one may expect a 45% efficiency and a background level of 1 event/Mt.y. So, for a 1 Mt.yr (10 yrs) exposure with GLACIER one reaches $\tau_p/B > 0.4\ 10^{35}$ yrs at 90% C.L.

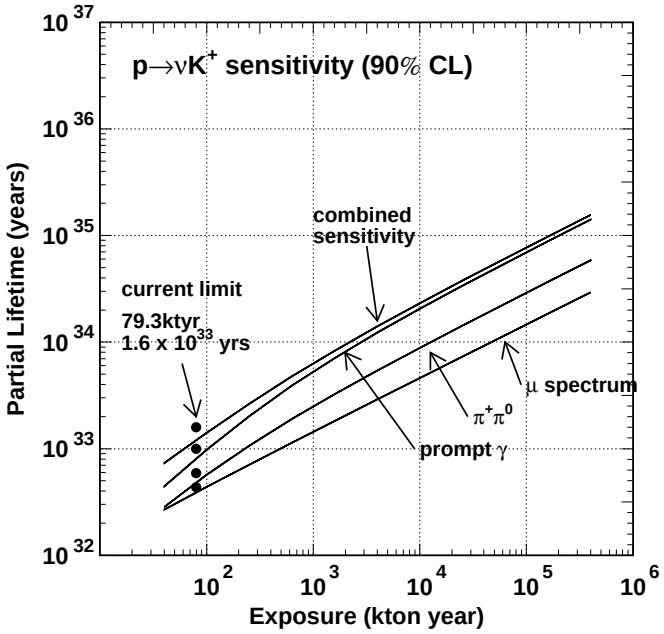

FIG. 7 Expected sensitivity on νK^+ proton decay as a function of MEMPHYS exposure (Jung, 2000) (see text for details).

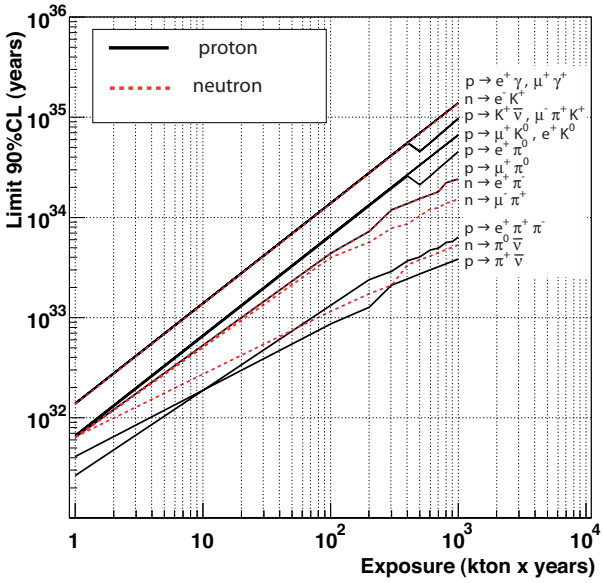

FIG. 8 Expected proton decay lifetime limits (τ/B at 90% C.L.) as a function of exposure for GLACIER. In this plot, only atmospheric neutrino background has been taken into account.

(see Fig. 8).

In a liquid scintillator detector the decay $p \rightarrow e^+\pi^0$ will produce a $\sim$ 938 MeV signal coming from e^+ and π^0 showers. Only atmospheric neutrinos are expected to cause background events in this energy range. Using the fact that showers from both e^+ and π^0 propagate $\sim$4 m in opposite directions before being stopped, atmospheric neutrino background can be reduced. Applying this method, the current limit for this channel ($\tau_p/B = 5.4\ 10^{33}$ y (Nakaya, 2005)) could be improved.

B. $p \rightarrow \overline{\nu} K^+$

In LENA, proton decay events via the mode $p \rightarrow K^+\overline{\nu}$ have a very clear signature. The kaon causes a prompt monoenergetic signal (T=105 MeV) and from the kaon decay there is a short-delayed second monoenergetic signal, bigger than the first one. The kaon has a lifetime of $\tau(K^+) = 12.8$ ns and two main decay channels: with a probability of 63.43 % it decays via $K^+ \rightarrow \mu^+\nu_\mu$ and with 21.13%, via $K^+ \rightarrow \pi^+\pi^0$.

Simulations of proton decay events and atmospheric neutrino background has been performed and a pulse shape analysis has been applied. From the analysis an efficiency of 65% for the detection of a possible proton decay has been determined and a background suppression of $\sim 2\ 10^4$ has been achieved (Marrodán Undagoitia *et al.*, 2005). A detail study of background implying pion and kaon production in atmospheric neutrino reactions has been performed leading to a background rate of 0.064 y^{-1} due to the reaction $\nu_\mu + p \rightarrow \mu^- + K^+ + p$.

For the current proton lifetime limit for the channel considered ($\tau_p/B = 2.3\ 10^{33}$ y) (Kobayashi *et al.*, 2005), about 40.7 proton decay events would be observed in LENA after a measuring time of ten years with less than 1 background event. If no signal is seen in the detector within this ten years, the lower limit for the lifetime of the proton will be placed at $\tau_p/B > 4\ 10^{34}$ y at 90% C.L.

For GLACIER, this is a quite clean channel due to the presence of a strange meson and no other particle in the final state. Using dE/dx versus range as discriminating variable in a Neural Net, we can determine the particle identity. We expect less than 1% of kaons mis-identified as protons. In this channel, the selection efficiency is high (97%) for a low atmospheric neutrino background < 1 event/Mt.y. In case of absence of signal and for a detector location at a depth of 1 km w.e., we expect for 1 Mt.y (10 years) exposure one event background due to cosmogenic sources. This translates into a limit $\tau_p/B > 0.6\ 10^{35}$ yrs at 90% C.L. This result remains valid even at shallow depths where cosmogenic background sources are a very important limiting factor for proton decay searches. A very large area annular active muon veto shield could be used in order to further suppress cosmogenic backgrounds at shallow depths. For example, the study done by (Bueno *et al.*, 2007) shows that a three plane active veto at a shallow depth of about 200 m rock overburden in the *under a hill configuration* yields similar sensitivity for $p \rightarrow K^+\bar{\nu}$ as a 3 km w.e. deep detector.

For the MEMPHYS detector, one should rely on the

TABLE IV Summary of the $e^+\pi^0$ and $\bar{\nu}K^+$ discovery potential by the three detectors. The $e^+\pi^0$ channel is not yet simulated in LENA.

	GLACIER	LENA	MEMPHYS
$e^+\pi^0$			
ϵ(%)/Bkgd(Mt.y)	45/1	-	43/2.25
τ_p/B (90% C.L., 10 yrs)	0.4×10^{35}	-	1.0×10^{35}
$\bar{\nu}K^+$			
ϵ(%)/Bkgd(Mt.y)	97/1	65/1	8.8/3
τ_p/B (90% C.L., 10 yrs)	0.6×10^{35}	0.4×10^{35}	0.2×10^{35}

detection of the decay products of the K^+ since its momentum (360 MeV) is below the water Čerenkov threshold (ie. 570 MeV): a 256 MeV/c muon and its decay electron (type I) or a 205 MeV/c π^+ and π^0 (type II), with the possibility of a delayed (12 ns) coincidence with the 6 MeV ^{15}N de-excitation prompt γ (Type III). Using the imaging and timing capability of Super-Kamiokande, the efficiency for the reconstruction of $p \rightarrow \overline{\nu}K^+$ is $\epsilon = 33\%$ (I), 6.8% (II) and 8.8% (III), and the background is at 2100, 22 and 6 events/Mt.yr level. For the prompt γ method, the background is dominated by misreconstruction. As stated by UNO, there are good reasons to believe that this background can be lowered by at least a factor 2 corresponding to the atmospheric neutrino interaction $\nu p \rightarrow \nu \Lambda K^+$. In these conditions, and using Super-Kamiokande performances, a 5 Mt.yr MEMPHYS exposure would allow to reach $\tau_p/B > 2\ 10^{34}$ yrs (see Fig. 7).

C. Comparison between the detectors

Preliminary comparisons have been done between the detectors (Tab. IV). For the $e^+\pi^0$ channel, the Čerenkov detector gets a better limit due to their higher mass. However it should be noted that GLACIER, although five times smaller in mass than MEMPHYS, gets an expected limit that is only a factor two smaller. Liquid argon TPCs and liquid scintillator detectors get better results for the $\bar{\nu}K^+$ channel, due to their higher detection efficiency. The two techniques look therefore quite complementary. We have also seen that GLAICER does not necessarily requires very deep underground laboratories, like those currently existing or future planned sites, to perform very sensitive nucleon decay searches.

V. SUPERNOVA NEUTRINOS

A supernova (SN) neutrino detection represents one of the next frontiers of neutrino astrophysics. It will provide invaluable information on the astrophysics of the core-collapse explosion phenomenon and on the neutrino mixing parameters. In particular, neutrino flavor transitions in the SN envelope are sensitive to the value of θ_{13} and on the type of mass hierarchy, and the detection of SN neutrino spectra at Earth can significantly contribute to sharpen our understanding of these unknown neutrino parameters. On the other hand, a detailed measurement of the neutrino signal from a galactic SN could yield important clues on the SN explosion mechanism.

A. SN neutrino emission and oscillations

A core-collapse supernova marks the evolutionary end of a massive star ($M \gtrsim 8\,M_\odot$) which becomes inevitably instable at the end of its life: it collapses and ejects its outer mantle in a shock-wave driven explosion. The collapse to a neutron star ($M \simeq M_\odot$, $R \simeq 10$ km) liberates a gravitational binding energy, $E_B \approx 3 \times 10^{53}$ erg, released at $\sim 99\%$ into (anti)neutrinos of all the flavors, and only at $\sim$1% into the kinetic energy of the explosion. Therefore, a core-collapse SN represents one of the most powerful sources of (anti)neutrinos in the Universe.

In general, numerical simulations of supernova explosions provide the original neutrino spectra in energy and time F^0_ν. Such initial distributions are in general modified by flavor transitions in SN envelope, in vacuum (and eventually in Earth matter)

$$F^0_\nu \longrightarrow F_\nu \tag{2}$$

and must be convolved with the differential interaction cross section σ_e for electron or positron production, as well as with the detector resolution function R_e, and the efficiency ε, in order to finally get observable event rates:

$$N_e = F_\nu \otimes \sigma_e \otimes R_e \otimes \varepsilon \tag{3}$$

Regarding the initial neutrino distributions F^0_ν, a SN collapsing core is roughly a black-body source of thermal neutrinos, emitted on a timescale of $\sim$ 10 s. Energy spectra parametrization are typically cast in the form of quasi-thermal distributions, with typical average energies: $\langle E_{\nu_e} \rangle = 9 - 12$ MeV, $\langle E_{\bar{\nu}_e} \rangle = 14 - 17$ MeV, $\langle E_{\nu_x} \rangle = 18 - 22$ MeV, where ν_x indicates any non-electron flavor.

The oscillated neutrino fluxes arriving at Earth may be written in terms of the energy-dependent "survival probability" p ($\bar{p}$) for neutrinos (antineutrinos) as (Dighe and Smirnov, 2000)

$$\begin{aligned} F_{\nu_e} &= pF^0_{\nu_e} + (1-p)F^0_{\nu_x} \\ F_{\bar{\nu}_e} &= \bar{p}F^0_{\bar{\nu}_e} + (1-\bar{p})F^0_{\nu_x} \\ 4F_{\nu_x} &= (1-p)F^0_{\nu_e} + (1-\bar{p})F^0_{\bar{\nu}_e} + (2+p+\bar{p})F^0_{\nu_x} \end{aligned} \tag{4}$$

where ν_x stands for either ν_μ or ν_τ. The probabilities p and $\bar{p}$ crucially depend on the neutrino mass hierarchy and on the unknown value of the mixing angle θ_{13} as shown in Tab. V.

TABLE V Values of the p and $\bar{p}$ parameters used in Eq. 4 in different scenario of mass hierarchy and $\sin^2\theta_{13}$.

Mass Hierarchy	$\sin^2\theta_{13}$	p	$\bar{p}$
Normal	$\gtrsim 10^{-3}$	0	$\cos^2\theta_{12}$
Inverted	$\gtrsim 10^{-3}$	$\sin^2\theta_{12}$	0
Any	$\lesssim 10^{-5}$	$\sin^2\theta_{12}$	$\cos^2\theta_{12}$

B. SN neutrino detection

Galactic core-collapse supernovae are rare, perhaps a few per century. Up to now, supernova neutrinos have been measured only once during SN 1987A explosion in the Large Magellanic Cloud ($d = 50$ kpc). Due to the relatively small masses of the detectors operative at that time, only few events were detected (11 in Kamiokande (Hirata *et al.*, 1987, 1988b) and 8 in IMB (Aglietta *et al.*, 1987; Bionta *et al.*, 1987)). The three proposed large-volume neutrino detectors with a broad range of science goals might guarantee continuous exposure for several decades, so that a high-statistics supernova neutrino signal may eventually be observed.

Expected number of events for GLACIER, MEMPHYS and LENA are reported in Tab. VI, for a typical galactic SN distance of 10 kpc. In the upper panel it is reported the total number of events, while the lower part refers to the ν_e signal detected during the prompt neutronization burst, with a duration of ~ 25 ms, just after the core bounce.

One can realize that $\bar{\nu}_e$ detection by Inverse β Decay (IβD) is the golden channel for MEMPHYS and LENA. In addition, the electron neutrino signal can be detected in LENA thanks to the interaction on ^{12}C. The three charged current reactions will deliver information on ν_e and $\bar{\nu}_e$ fluxes and spectra while the three neutral current reactions, sensitive to all neutrino flavours will provide information on the total flux. GLACIER has also the opportunity to see the ν_e by charged current interactions on ^{40}Ar with a very low threshold. The detection complementarity between ν_e and $\bar{\nu}_e$ is of great interest and would assure a unique way to probe SN explosion mechanism as well as neutrino intrinsic properties. Moreover, the huge statistics would allow spectral studies in time and in energy domain.

We stress that it will be difficult to establish SN neutrino oscillation effects solely on the basis of a $\bar{\nu}_e$ or ν_e "spectral hardening" relative to theoretical expectations. Therefore, in the recent literature the importance of model-independent signatures has been emphasized. Here we focus mainly on the signatures associated to: the prompt ν_e neutronization burst, the shock-wave propagation, the Earth matter crossing.

The analysis of the time structure of the SN signal during the first few tens of milliseconds after the core bounce can provide a clean indication if the full ν_e burst is present or absent and therefore allows one to distinguish between different mixing scenarios as indicated by the third column of Tab. VII. For example, if the mass ordering is normal and the θ_{13} is large, the ν_e burst will fully oscillate into ν_x. If θ_{13} is measured in the laboratory to be large, for example by one of the forthcoming reactor experiments, then one may distinguish between the normal and inverted mass ordering.

As discussed, MEMPHYS is mostly sensitive to the IβD, although the ν_e channel can be measured by the elastic scattering reaction $\nu_x + e^- \to e^- + \nu_x$ (Kachelriess *et al.*, 2005). Of course, the identification of the neutronization burst is cleanest with a detector using the charged-current absorption of ν_e neutrinos, like GLACIER. Using its unique features to look at ν_e CC it is possible to probe oscillation physics during the early stage of the SN explosion, and using the NC it is possible to decouple the SN mechanism from the oscillation physics (Gil-Botella and Rubbia, 2003, 2004).

A few seconds after core bounce, the SN shock wave will pass the density region in the stellar envelope relevant for oscillation matter effects, causing a transient modification of the survival probability and thus a time-dependent signature in the neutrino signal (Fogli *et al.*, 2003; Schirato *et al.*, 2002). It would show a characteristic dip when the shock wave passes (Fogli *et al.*, 2005), or a double-dip feature if a reverse shock occurs (Tomas *et al.*, 2004). The detectability of such a signature has been studied in a Megaton Water Čerenkov detector like MEMPHYS by the IβD (Fogli *et al.*, 2005), and in a Large liquid Argon detector like GLACIER by Ar CC interactions (Barger *et al.*, 2005). The shock wave effects would be certainly visible also in a large volume scintillator like LENA. Of course, apart from identifying the neutrino mixing scenario, such observations would test our theoretical understanding of the core-collapse SN phenomenon.

One unequivocal indication of oscillation effects would be the energy-dependent modulation of the survival probability $p(E)$ caused by Earth matter effects (Lunardini and Smirnov, 2001). The Earth matter effects can be revealed by wiggles in energy spectra and LENA benefit from a better energy resolution than MEMPHYS in this respect which may be partially compensated by 10 times more statistics (Dighe *et al.*, 2003b). The Earth effect would show up in the $\bar{\nu}_e$ channel for the normal mass hierarchy, assuming that θ_{13} is large (Tab. VII). Another possibility to establish the presence of Earth effects is to use the signal from two detectors if one of them sees the SN shadowed by the Earth and the other not. A comparison between the signal normalization in the two detectors might reveal Earth effects (Dighe *et al.*, 2003a). The shock wave propagation can influence the Earth matter effect, producing a delayed effect $5 - 7$ s after the core-bounce, in some particular situations (Lunardini and Smirnov, 2003) (Tab. VII).

Exploiting these three experimental signatures, by the joint efforts of the complementarity SN neutrino detection in MEMPHYS, LENA, and GLACIER it would be possible to extract valuable information on the neutrino

TABLE VI Summary of the expected neutrino interaction rates in the different detectors for a $8M_{\odot}$ SN located at 10 kpc (Galactic center). The following notations have been used: IβD, eES and pES stands for Inverse β Decay, electron and proton Elastic Scattering, respectively. The final state nuclei are generally unstable and decay either radiatively (notation *), or by β^-/β^+ weak interaction (notation $^{\beta^-,^+}$). The rates of the different reaction channels are listed, and for LENA they have been obtained by scaling the predicted rates from (Beacom *et al.*, 2002; Cadonati *et al.*, 2002).

MEMPHYS		LENA		GLACIER	
Interaction	Rates	Interaction	Rates	Interaction	Rates
$\bar{\nu}_e$ IβD	2×10^5	$\bar{\nu}_e$ IβD	9×10^3	$\nu_e^{CC}(^{40}Ar, ^{40}K^*)$	2.5×10^4
$\overset{(-)}{\nu}_e^{CC}(^{16}O, X)$	10^4	ν_x pES	7×10^3	$\nu_x^{NC}(^{40}Ar^*)$	3.0×10^4
ν_x eES	10^3	$\nu_x^{NC}(^{12}C^*)$	3×10^3	ν_x eES	10^3
		ν_x eES	600	$\bar{\nu}_e^{CC}(^{40}Ar, ^{40}Cl^*)$	540
		$\bar{\nu}_e^{CC}(^{12}C, ^{12}B^{\beta^+})$	500		
		$\nu_e^{CC}(^{12}C, ^{12}N^{\beta^-})$	85		
Neutronization Burst rates					
MEMPHYS	60	ν_e eES			
LENA	70	ν_e eES/pES			
	$\nu_e^{CC}(^{12}C, ^{12}N^{\beta^-})$				
GLACIER	380	$\nu_x^{NC}(^{40}Ar^*)$			

mass hierarchy and to put a bound on θ_{13}, as shown in Tab. VII.

As an important caveat we mention that very recently it has been recognized that nonlinear oscillation effects caused by neutrino-neutrino interactions can have a dramatic impact on the neutrino flavor evolution for approximately the first 100 km above the neutrino sphere (Duan *et al.*, 2006; Hannestad *et al.*, 2006). The impact of these novel effects on the observable oscillation signatures has not yet been systematically studied. Therefore, our description of observable oscillation effects may need revision in future as a better understanding of the consequences of these nonlinear effects develops.

Other interesting ideas has been also studied in the literature, ranging from the pointing of a SN by neutrinos (Tomas *et al.*, 2003), determining its distance from the deleptonization burst that plays the role of a standard candle (Kachelriess *et al.*, 2005), an early alert for SN observatory exploiting the neutrino signal (Antonioli *et al.*, 2004), and the detection of neutrinos from the last phases of a burning star (Odrzywolek *et al.*, 2004).

Up to now, we have investigated SN in our Galaxy, but the calculated rate of supernova explosions within a distance of 10 Mpc is about 1 per year. Although the number of events from a single explosion at such large distances would be small, the signal could be separated from the background with the request to observe at least two events within a time window comparable to the neutrino emission time-scale ($\sim$ 10 sec), together with the full energy and time distribution of the events (Ando *et al.*, 2005). In a MEMPHYS detector, with at least two neutrinos observed, a supernova could be identified without optical confirmation, so that the start of the light curve could be forecasted by a few hours, along with a short list of probable host galaxies. This would also allow the detection of supernovae which are either heavily obscured by dust or are optically dark due to prompt black hole formation.

C. Diffuse Supernova Neutrino Background

A galactic Supernova explosion will be a spectacular source of neutrinos, so that a variety of neutrino and SN properties could be determined. However, only one such explosion is expected in 20 to 100 years. Alternatively, it has been suggested that we might detect the cumulative neutrino flux from all the past SN in the Universe, the so called Diffuse Supernova Neutrino (DSN) Background[2]. In particular, there is an energy window around $10 - 40$ MeV where the DSN signal can emerge above other sources, so that proposed detectors may measure this flux after some years of exposure times.

The DSN signal, although weak, is not only "guaranteed", but can also probe physics different from that of a galactic SN, including processes which occur on cosmological scales in time or space.

For instance, the DSN signal is sensitive to the evolution of the SN rate (SNR), which is closely related to the star formation rate (Ando, 2004; Fukugita and Kawasaki, 2003). Additionally, neutrino decay scenarios with cosmological lifetimes could be analyzed and constrained (Ando, 2003) as proposed in (Fogli *et al.*, 2004).

An upper limit on the DSN flux has been set by the

[2] We prefer the word "Diffuse" rather than "Relic" not to confuse with the primordial neutrinos produced one second after the Big Bang.

TABLE VII Summary of the neutrino properties effect on ν_e and $\bar{\nu}_e$ signals.

Mass Hierarchy	$\sin^2\theta_{13}$	ν_e neutronization peak	Shock wave	Earth effect
Normal	$\gtrsim 10^{-3}$	Absent	ν_e	$\bar{\nu}_e$ ν_e (delayed)
Inverted	$\gtrsim 10^{-3}$	Present	$\bar{\nu}_e$	ν_e $\bar{\nu}_e$ (delayed)
Any	$\lesssim 10^{-5}$	Present	-	both $\bar{\nu}_e$ ν_e

TABLE VIII DSN expected rates. The larger numbers are computed with the present limit on the flux by SuperKamiokande collaboration. The lower numbers are computed for typical models. The background coming from reator plants have been computed for specific locations for MEMPHYS and LENA. For MEMPHYS, the SuperKamiokande background has been scaled by the exposure. More studies are needed to estimate the background at the new Fréjus laboratory.

Interaction	Exposure	Energy Window	Signal/Bkgd
1 shaft MEMPHYS + 0.2% Gd (with bkgd Kamioka)			
$\bar{\nu}_e + p \rightarrow n + e^+$ $n + Gd \rightarrow \gamma$ (8 MeV, 20 μs)	0.7 Mt.y 5 yrs	$[15-30]$ MeV	(43-109)/47
LENA at Pyhäsalmi			
$\bar{\nu}_e + p \rightarrow n + e^+$ $n + p \rightarrow d + \gamma$ (2 MeV, 200 μs)	0.4 Mt.y 10 yrs	$[9.5-30]$ MeV	(20-230)/8
GLACIER			
$\nu_e + {}^{40}Ar \rightarrow e^- + {}^{40}K^*$	0.5 Mt.y 5 yrs	$[16-40]$ MeV	(40-60)/30

SuperKamiokande experiment (Malek *et al.*, 2003)

$$\phi^{\rm DSN}_{\bar{\nu}_e} < 1.2 {\rm cm}^{-2}\ {\rm s}^{-1} (E_\nu > 19.3\ {\rm MeV}) \qquad (5)$$

However most of the predictions are below this limit and therefore DSN detection appears to be feasible only with the large detector foreseen, through $\bar{\nu}_e$ inverse beta decay in MEMPHYS and LENA detectors and through $\nu_e + {}^{40}Ar \rightarrow e^- + {}^{40}K^*$ (and the associated gamma cascade) in GLACIER (Cocco *et al.*, 2004).

Typical estimates for DSN fluxes (see for example (Ando, 2004)) predict an event rate of the order of $(0.1-0.5)$ cm^{-2} s^{-1} MeV^{-1} for energies above 20 MeV.

The DSN signal energy window is constrained from above by the atmospheric neutrinos and from below by either the nuclear reactor $\bar{\nu}_e$ (I), the spallation production of unstable radionuclei by cosmic ray muons (II), the decay of "invisible" muons into electrons (III), and solar ν_e neutrinos (IV). The three detectors are affected differently by these backgrounds.

GLACIER looking at ν_e is mainly affected by type IV. MEMPHYS filled with pure water is mainly affected by type III due to the fact that the muons may have not enough energy to produce Čerenkov light. As pointed out in (Fogli *et al.*, 2005) with the addition of Gadolinium (Beacom and Vagins, 2004) the detection of the captured neutron releasing 8 MeV gamma after ~ 20 μs (10 times faster than in pure water) would give the possibility to reject the "invisible" muon (type III) as well as spallation background (type II). LENA taking benefit from the delayed neutron capture in $\bar{\nu}_e + p \rightarrow n + e^+$, is mainly affected by reactor neutrinos (I) which impose to choose an underground site far from nuclear plants: if LENA is deployed at the Center for Underground Physics in Pyhäsalmi (CUPP, Finland), there will be an observational window from ~ 9.7 to 25 MeV that is almost free of background. The expected rates of signal and background are presented in Tab. VIII.

According to current DSN models (Ando, 2004) that are using different SN simulations from the LL (Totani *et al.*, 1998), TBP (Thompson *et al.*, 2003) and KRJ (Keil *et al.*, 2003) groups for the prediction of the DSN energy spectrum and flux, a detection of $\sim$10 DSN events per year is expected in LENA. Signal rates corresponding to three different DSN models and the background rates due to the reactor (I) and atmospheric neutrinos are shown in Fig. 9 for 10 years of measurement with LENA in CUPP.

Apart from mere detection, spectroscopy of the DNS events in LENA will constrain the parameter space of core-collapse models. If the SNR signal is known at a sufficient precision, the spectral slope of the DSN can be used to determine the hardness of the initial SN neutrino spectrum. For the currently favoured value of the SNR,

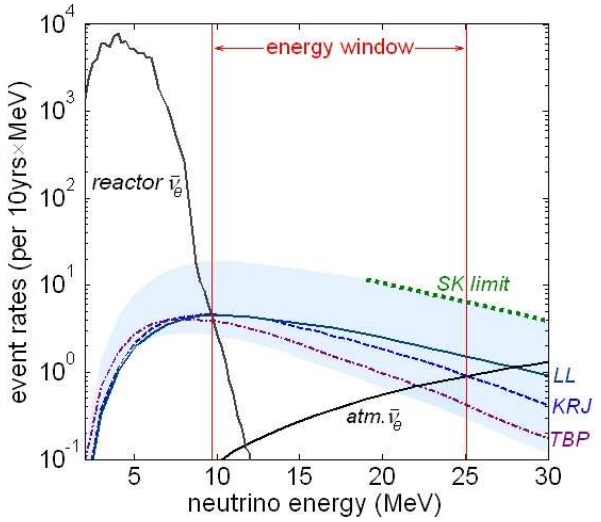

FIG. 9 Diffuse supernova neutrino signal and background in LENA detector in 10 years of exposure. Shaded regions give the uncertainties of all curves. An observational window between ~ 9.5 to 25 MeV that is almost free of background can be identified (for the Pyhäsalmi site) (Wurm *et al.*, 2006).

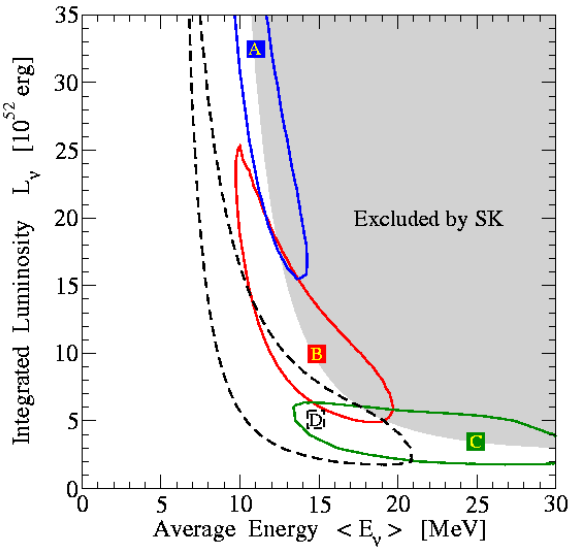

FIG. 10 Possible 90% C.L. measurements of the emission parameters of supernova electron antineutrino emission after 5 years running of a gadolinium-enhanced SK detector or 1 year of one gadolinium-enhanced MEMPHYS shaft (Yuksel *et al.*, 2006).

the discrimination between the discussed LL and TBP core-collapse models will be possible at 2.6σ after 10 years of measuring time (Wurm *et al.*, 2006).

In addition, by an analysis of the flux in the energy region from 10 to 14 MeV the SNR for $z < 2$ could be constrained at high significance levels, as in this energy regime the DSN flux is only weakly dependent on the assumed SN model. This could be used to cross-check FIR and UV measurements.

The detection of the redshifted DSN from $z > 1$ is limited by the flux of the reactor $\bar{\nu}_e$ background. In Pyhasalmi, a lower threshold of 9.5 MeV resuls in a spectral contribution of 25% DSN from $z > 1$.

An analysis of the expected DSN spectrum that would be observed with a gadolinium-loaded Water Čerenkov detector has been carried out in (Yuksel *et al.*, 2006). The possible measurements of the parameters (integrated luminosity and average energy) of supernova $\bar{\nu}_e$ emission have been computed for 5 years running of a Gd-enhanced SuperKamiokande detector, which would correspond to 1 year of one Gd-enhanced MEMPHYS shaft. The results are shown in Fig. 10. Even if detailed studies on characterization of the background are needed, the DSN events may be as powerful as the measurement made by Kamioka and IMB with the SN1987A $\bar{\nu}_e$ events.

VI. SOLAR NEUTRINOS

In the past years Water Čherenkov detectors have measured the high energy tail ($E > 5$ MeV) of the solar ^{8}B neutrino flux using electron-neutrino elastic scattering (Smy, 2003). Since such detectors could record the time of an interaction and reconstruct the energy and direction of the recoiling electron, unique information of the spectrum and time variation of the solar neutrino flux was extracted. This provided further insights into the "solar neutrino problem", the deficit of the neutrino flux (measured by several experiments) with respect to the flux expected by the standard solar models. It also constrained the neutrino flavor oscillation solutions in a fairly model-independent way.

With MEMPHYS, Super-Kamiokande's measurements obtained from 1258 days of data could be repeated in about half a year (the seasonal flux variation measurement requires of course a full year). In particular, a first measurement of the flux of the rare "hep" neutrinos may be possible. Elastic neutrino-electron scattering is strongly forward peaked. To separate the solar neutrino signal from the isotropic background events (mainly due to low radioactivity), this directional correlation is exploited. Angular resolution is limited by multiple scattering. The reconstruction algorithm first reconstructs the vertex from the PMT times and then the direction assuming a single Cherenkov cone originating from the reconstructed vertex. Reconstructing 7 MeV events in MEMPHYS seems not to be a problem but decreasing the threshold would imply serious care of the PMT dark current rate as well as the laboratory and detector radioactivity level.

With LENA, a large amount of neutrinos from ^{7}Be, around $\sim 5.4 \times 10^3$/day ($\sim 2.0 \times 10^6$/y) would be detected. Depending on the signal-to-background ratio, this would provide a sensitivity for time variations in the ^{7}Be neutrino flux of $\sim 0.5\%$ during one month of measuring time. Such a sensitivity may give information at a unique level on helioseismology (pressure or temperature

fluctuations in the center of the sun) and on a possible magnetic moment interaction with a timely varying solar magnetic field.

The *pep* neutrinos are expected to be recorded at a rate of 210/day ($\sim 7.7 \times 10^4$/y), these neutrinos would provide a better understanding of the global solar neutrino luminosity. Due to the value of their energy, they could probe the transition region of vacuum to matter-dominated neutrino oscillation.

The neutrino flux from the CNO cycle is theoretically predicted with the lowest accuracy (30%) of all solar neutrino fluxes. Therefore, LENA would provide a new opportunity for a detailed study of solar physics. However, the observation of such solar neutrinos in these detectors, i.e. through elastic scattering, is not a simple task, since neutrino events cannot be separated from the background, and it can be accomplished only if the detector contamination will be kept very low (Alimonti *et al.*, 1998a,b). Moreover, only mono-energetic sources as such mentioned can be detected, taking advantage of the Compton-like shoulder edge produced in the event spectrum.

Recently, the possibility to register ^{8}B solar neutrinos by means of the charged current interaction with the ^{13}C (Ianni *et al.*, 2005) nuclei naturally contained in organic scintillators has been investigated. Even if the event signal does not keep the directionality of the neutrino, it can be separated from the background by exploiting the time and space coincidence with the subsequent decay of the produced ^{13}N nuclei (remaining background of about 60/year corresponding to a reduction factor of $\sim 3\ 10^{-4}$) (Ianni *et al.*, 2005). Around 360 events of this type per year can be estimated for LENA. A deformation due to the MSW-effect should be observable in the low-energy regime after a couple of years of measurements.

For the proposed location of LENA in Pyhäsalmi ($\sim$ 4000 m.w.e.), the cosmogenic background will be sufficiently low for the mentioned measurements. Notice that Fréjus site would also be adequate for this topic ($\sim$ 4800 m.w.e.). The radioactivity of the detector would have to be kept very low (10^{-17} g/g level U-Th) as in the KamLAND detector.

The solar neutrinos in GLACIER can be registered through the elastic scattering $\nu_x + e^- \rightarrow \nu_x + e^-$ (ES) and the absorption reaction $\nu_e + {}^{40}Ar \rightarrow e^- + {}^{40}K^*$ (ABS) followed by γs emission. Even if these reactions have low threshold (e.g 1.5 MeV for the second one), one expects to operate in practice with a threshold set at 5 MeV on the primary electron kinetic energy to reject background from neutron capture followed by gamma ray emission which constitute the main background in some underground laboratory (Arneodo *et al.*, 2001) as for the LNGS (Italy). These neutrons are induced by the spontaneous fission of the cavern rock (note that in case of a salt mine this background may be significantly reduced).

The expected raw event rate is 330,000/year (66% from ABS, 25% from ES and 9% from neutron background induced events) assuming the above mentioned threshold on the final electron energy. Then, applying further offline cuts to purify separatly the ES sample and the ABS sample, one gets the rates shown on Tab. IX.

TABLE IX Number of events expected in GLACIER per year, compared with the computed background (no oscillation) in the Gran Sasso Laboratory (Italy) rock radioactivity condition (i.e. 0.32 10^{-6} n cm^{-2} s^{-1}($>$ 2.5 MeV). The Absorption channel have been split into the contributions of events from Fermi transition and from Gamow-Teller transition of the ^{40}Ar to the different ^{40}K excited levels and that can be separated using the emitted gamma energy and multiplicity

	Events/year
Elastic channel ($E \geq 5$ MeV)	45,300
Neutron bkgd	1,400
Absorption events contamination	1,100
Absorption channel (Gamow-Teller transition)	101,700
Absorption channel (Fermi transition)	59,900
Neutron bkgd	5,500
Elastic events contamination	1,700

A possible way to combine the ES and the ABS channels similar to the NC/CC flux ratio measured by SNO collaboration (Aharmim *et al.*, 2005), is to compute the following ratio:

$$R = \frac{N^{ES}/N_0^{ES}}{\frac{1}{2}\left(N^{Abs-GT}/N_0^{Abs-GT} + N^{Abs-F}/N_0^{Abs-F}\right)} \quad (6)$$

where the numbers of expected events without neutrino oscillations are labeled with a 0). This double ratio has the following advantages: first it is independent of the ^{8}B total neutrino flux, predicted by different solar models, and second it is free of experimental threshold energy bias and of the adopted cross-sections for the different channels. With the present fit to solar and KamLAND data, one expects a value of $R = 1.30 \pm 0.01$ after one year of data taking with GLACIER. The quoted error for R only takes into account statistics.

VII. ATMOSPHERIC NEUTRINOS

A. Introduction

Atmospheric neutrinos originates from the decay chain initiated by the collision of cosmic rays with the upper layers of the Earth's atmosphere. The hadronic interaction between primary cosmic rays (mainly protons and helium nuclei) and the light atmosphere nuclei produces secondary π and K mesons, which then decay giving electron and muon neutrinos and antineutrinos. At lower energies the main contribution comes from π mesons, and the decay chain $\pi \rightarrow \mu + \nu_\mu$ followed by $\mu \rightarrow e + \nu_e + \nu_\mu$ produces essentially two ν_μ for each ν_e. As the energy

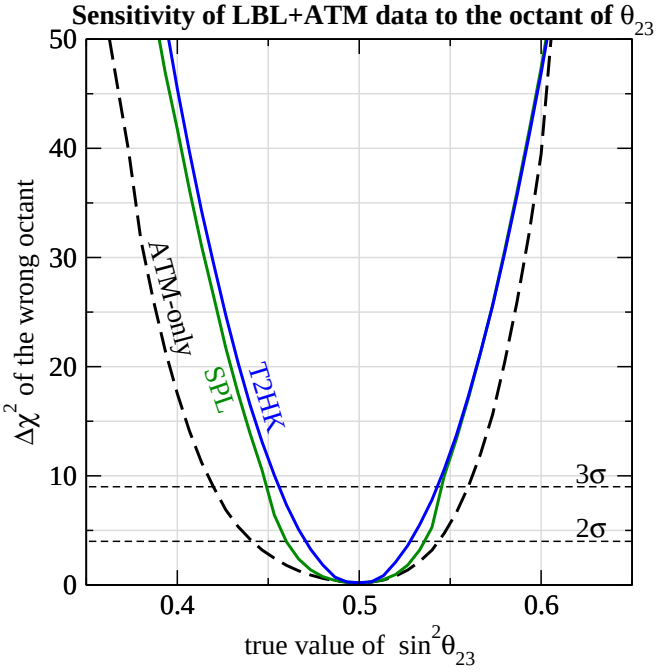

FIG. 11 Discrimination of the wrong octant solution as a function of $\sin^2\theta_{23}^{\rm true}$, for $\theta_{13}^{\rm true} = 0$. We have assumed 10 years of data taking with a 440-kton detector.

increases, more and more muons reach the ground before decays, and therefore the ν_μ/ν_e ratio increases. For $E_\nu \gtrsim 1$ GeV the dependence of the total neutrino flux on the neutrino energy is well described by a power law, $d\Phi/d_E \propto E^{-\gamma}$ with $\gamma = 3$ for ν_μ and $\gamma = 3.5$ for ν_e, whereas at sub-GeV energies the dependence becomes more complicated because of the effects of the solar wind and of the Earth's magnetic field (Gonzalez-Garcia and Nir, 2003). As for the zenith dependence, for energies larger than a few GeV the neutrino flux is enhanced in the horizontal direction since pions and muons can travel a longer distance before reaching the ground, and therefore have more chances to decay producing neutrinos.

Historically, the atmospheric neutrino problem originated in the 1980's as a discrepancy between the atmospheric neutrino flux measured with different experimental techniques. In the previous years, a number of detectors had been built, which could detect neutrinos through the observation of the charged lepton produced in charged-current neutrino-nucleon interactions inside the detector itself. These detectors could be divided into two classes: *iron calorimeters*, which reconstructed the track or electromagnetic shower produced by the lepton, and *water Čerenkov*, which measured instead the Cerenkov light emitted by the lepton as it moved faster than light in water. The oldest iron calorimeters, Frejus (Daum *et al.*, 1995) and NUSEX (Aglietta *et al.*, 1989), found no discrepancy between the observed flux and the theoretical predictions, whereas the two Water Čerenkov detectors, IMB (Becker-Szendy *et al.*, 1992) and Kamiokande (Hirata *et al.*, 1992), observed a clear deficit in the predicted ν_μ/ν_e ratio. The problem was finally solved in 1998, when the water Cerenkov detector SuperKamiokande (Fukuda *et al.*, 1998) established with high statistical accuracy that there was indeed a zenith- and energy-dependent deficit in the muon neutrino flux with respect to the theoretical predictions, and that this deficit was compatible with the hypothesis of mass-induced $\nu_\mu \to \nu_\tau$ oscillations. Also, the independent confirmation of this effect from the iron calorimeter experiments Soudan-II (Allison *et al.*, 1999) and MACRO (Ambrosio *et al.*, 2001) eliminated the discrepancy between the two experimental techniques.

Despite providing the first solid evidence for neutrino oscillations, atmospheric neutrino experiments have received only minor consideration during the last years. This is mainly due to two important limitations:

- the sensitivity of an atmospheric neutrino experiments is strongly limited by the large uncertainties in the knowledge of neutrino fluxes and neutrino-nucleon cross-section. Such uncertainties can be as large as 20%.
- in general, water Cerenkov detectors do not allow an accurate reconstruction of the neutrino energy and direction if none of the two is known "a priori". This strongly limits the sensitivity to Δm^2, which is very sensitive to the resolution on L/E.

During its phase-I, Super-Kamiokande has collected 4099 electron-like and 5436 muon-like contained neutrino events (Ashie *et al.*, 2005). With only about a hundred events each, K2K (Ahn *et al.*, 2006) and MINOS (Tagg, 2006) already provide a stronger bound on the atmospheric mass-squared difference Δm^2_{31}. The present value of the mixing angle θ_{23} is still dominated by Super-Kamiokande data, being statistics the most important factor for such a measurement, but strong improvements are expected from the next generation of long-baseline experiments T2K (Itow *et al.*, 2001) and NOνA (Ayres *et al.*, 2004).

B. Oscillation physics

Despite these drawbacks, atmospheric detectors can still play a leading role in the future of neutrino physics due to the huge range in energy (from 100 MeV to 10 TeV and above) and distance (from 20 km to more than 12000 Km) covered by the data. This unique feature, as well as the very large statistics expected for a detector such as MEMPHYS ($20 \div 30$ times the present SK event rate), will allow a very accurate study of *subdominant modifications* to the leading oscillation pattern, thus providing complementary information to accelerator-based experiments. More concretely, atmospheric neutrino data will be extremely valuable for:

- resolving the octant ambiguity: although future LBL experiments are expected to considerably improve the measurement of the absolute value of the

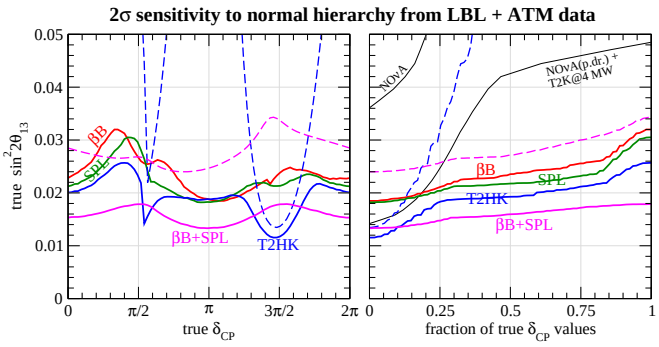

FIG. 12 Sensitivity to the mass hierarchy at 2σ ($\Delta\chi^2 = 4$) as a function of $\sin^2 2\theta_{13}^{\rm true}$ and $\delta_{\rm CP}^{\rm true}$ (left), and the fraction of true values of $\delta_{\rm CP}^{\rm true}$ (right). The solid curves are the sensitivities from the combination of long-baseline and atmospheric neutrino data, the dashed curves correspond to long-baseline data only. We have assumed 10 years of data taking with a 440-kton detector.

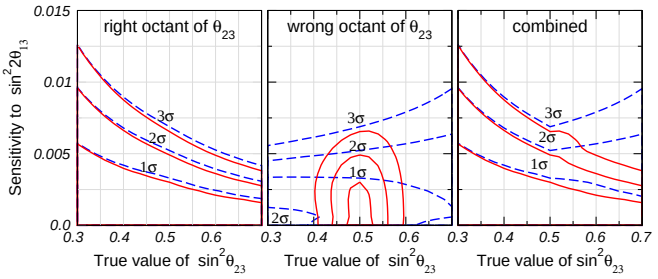

FIG. 13 Sensitivity to $\sin^2 2\theta_{13}$ as a function of $\sin^2\theta_{23}^{\rm true}$ for LBL data only (dashed), and the combination LBL+ATM (solid). In the left and central panels we restrict the fit of θ_{23} to the octant corresponding to $\theta_{23}^{\rm true}$ and $\pi/2 - \theta_{23}^{\rm true}$, respectively, whereas the right panel shows the overall sensitivity taking into account both octants. We have assumed 8 years of LBL and 9 years of ATM data taking with the T2HK beam and a 1 Mton detector.

small quantity $D_{23} \equiv \sin^2\theta_{23} - 1/2$, they will have practically no sensitivity on its sign. On the other hands, it has been pointed out (Kim and Lee, 1998; Peres and Smirnov, 1999) that the $\nu_\mu \to \nu_e$ conversion signal induced by the small but finite value of Δm^2_{21} can resolve this degeneracy. However, observing such a conversion requires a very long baseline and low energy neutrinos, and atmospheric sub-GeV electron-like events are particularly suitable for this purpose. In Fig. 11 we show the potential of different ATM+LBL experiments to exclude the octant degenerate solution.

- resolving the hierarchy degeneracy: if θ_{13} is not too small, matter effect will produce resonant conversion in the $\nu_\mu \leftrightarrow \nu_e$ channel for neutrinos (antineutrinos) if the mass hierarchy is normal (inverted). The observation of this enhanced conversion would allow the determination of the mass hierarchy. Although a magnetized detector would be the best solution for this task, it is possible to extract useful information also with a conventional detector since the event rates expected for atmospheric neutrinos and antineutrinos are quite different. This is clearly visible from Fig. 12, where we show how the sensitivity to the mass hierarchy of different LBL experiments is drastically increased when the ATM data collected by the same detector are also included in the fit.

- measuring or improving the bound on θ_{13}: although atmospheric data alone are not expected to be competitive with the next generation of long-baseline experiments in the sensitivity to θ_{13}, they will contribute indirectly by eliminating the octant degeneracy, which is an important source of uncertainty for LBL. In particular, if $\theta_{23}^{\rm true}$ is larger than 45° then the inclusion of atmospheric data will considerably improve the LBL sensitivity to θ_{13}, as can be seen from the right panel of Fig. 13 (Huber *et al.*, 2005).

C. Direct detection of ν_τ in the atmospheric neutrino flux

At energies above a GeV, we expect unoscillated events to be upward-downward going symmetric. In contrast, we know that ν_τ, $\bar\nu_\tau$ induced events come from below the horizon (upward going events). Therefore the presence of ν_τ, $\bar\nu_\tau$ events can be revealed by a measured excess of upward going events. Hereafter we assume that the ν_μ and the ν_τ are maximally mixed and their mass squared difference is $\Delta m^2 = 3. \times 10^{-3}$ eV^2. We use the Fluka 3D atmospheric neutrino fluxes.

In GLACIER, the search for ν_τ appearance is based on the information provided by the event kinematics and takes advantage of the special characteristics of ν_τ CC and the subsequent decay of the produced τ lepton when compared to CC and NC interactions of ν_μ and ν_e, i.e. by making use of $\vec{P}_{candidate}$ and $\vec{P}_{hadron}$. Due to the large background induced by the natural abundance of the atmospheric neutrino flux in ν_e and $\bar\nu_e$, we note that the measurement of a statistically significant excess of ν_τ events is very unlikely for the $\tau \to e$ decay mode, therefore we conclude that a search based on this channel is hopeless. Same conclusions apply to the muonic decay channel.

The situation is much more advantageous for the hadronic channels: we consider tau decays to one prong (single pion, rho) and to three prongs ($\pi^\pm\pi^0\pi^0$ and three charged pions). After a careful evaluation of the performance of different combinations of kinematic variables, we decided to use: $E_{visible}$, y_{bj} (the ratio between the total hadronic energy and $E_{visible}$) and Q_T (defined as the transverse momentum of the τ candidate with respect to the total measured momentum). The chosen variables are not independent one from another but show correlations between them. These correlations can be exploited

TABLE X Expected background and signal events for different combinations of the π, ρ and 3π analyses. The considered statistical sample corresponds to an exposure of 100 kton×year. The best combination found is indicated in bold characters.

$\ln\lambda_\pi$ Cut	$\ln\lambda_\rho$ Cut	$\ln\lambda_{3\pi}$ Cut	Top Events	Bottom Events	P_β (%)
0.	0.5	0.	223	$223+43=266$	2×10^{-1} (3.1σ)
1.5.	1.5	0	92	$92+35=127$	2×10^{-2} (3.7σ)
3.	-1	0.	87	$87+33=120$	3×10^{-2} (3.6σ)
3.	0.5	0.	25	$25+22=47$	2×10^{-3} (4.3σ)
3.	1.5	0	20	$20+19=39$	4×10^{-3} (4.1σ)
3.	0.5	-1.	59	$59+30=89$	9×10^{-3} (3.9σ)
3.	0.5	1.	18	$18+17=35$	1×10^{-2} (3.8σ)

to reduce the background. In order to maximize the separation between signal and background, we use three dimensional likelihood functions $\mathcal{L}(Q_T, E_{visible}, y_{bj})$ where correlations are taken into account. For every channel, we build three dimensional likelihood functions for both signal ($\mathcal{L}^S_\pi$, $\mathcal{L}^S_\rho$, $\mathcal{L}^S_{3\pi}$) and background ($\mathcal{L}^B_\pi$, $\mathcal{L}^B_\rho$, $\mathcal{L}^B_{3\pi}$). To enhance the separation of ν_τ induced events from ν_μ, ν_e interactions, we take a ratio of likelihoods as the sole discriminant variable:

$$\ln\lambda_i \equiv \ln(\mathcal{L}^S_i/\mathcal{L}^B_i) \tag{7}$$

where $i=\pi,\ \rho,\ 3\pi$.

To further improve the sensitivity of the ν_τ appearance search, we combine the three independent hadronic analyses into a single one. Events that are common to at least two analyses are counted only once and a survey of all possible combinations, for a restricted set of values of the likelihood ratios, is performed. Table X illustrates the statistical significance achieved by several selected combinations of the likelihood ratios for an exposure equivalent to 100 kton×year.

The best combination, for a 100 kton×year exposure, is achieved for the following set of cuts: $\ln\lambda_\pi > 3$, $\ln\lambda_\rho > 0.5$ and $\ln\lambda_{3\pi} > 0$. The expected number of NC background events amounts to 25 (top) while 25+22 = 47 (bottom) are expected. P_β is the Poisson probability for the measured excess of upward going events to be due to a statistical fluctuation as a function of the exposure. We have an effect larger than 4σ for an exposure of 100 kton×year (one year of data taking with GLACIER).

D. New phenomena beyond the "Standard Model"

It is worth remembering that atmospheric neutrino fluxes are themselves an important subject of investigation, and at the light of the precise determination of the oscillation parameters provided by long-baseline experiments the atmospheric neutrino data accumulated by the proposed detectors can be used as a *direct measurement* of the incoming neutrino flux, and therefore as an indirect measurement of the primary cosmic rays flux.

The appearance of subleading features in the main oscillation pattern can also be a hint for New Physics. The huge range of energies probed by atmospheric data will allow to put very strong bounds on mechanisms which predict deviation from the $1/E$ behavior. For example, the bound on non-standard neutrino-matter interactions and on other types of New Physics (such as violation of the equivalence principle, or violation of the Lorentz invariance) which can be derived from *present* data is already the strongest which can be put on these mechanisms (Gonzalez-Garcia and Maltoni, 2004). So, the increased statistics expected for the proposed detectors will further improve these constraints.

VIII. GEONEUTRINOS

The total power dissipated from the Earth (heat flow) has been measured with thermal techniques to be 44.2 ± 1.0 TW. Despite this small quoted error, a more recent evaluation of the same data (assuming much lower hydrothermal heat flow near mid-ocean ridges) has led to a lower figure of 31 ± 1 TW.

On the basis of studies of chondritic meteorites the calculated radiogenic power is thought to be 19 TW (about half of the total power), 84% of which is produced by ^{238}U and ^{232}Th decay which in turn produce $\bar\nu_e$ by β decays (geoneutrinos). It is then of prime importance to measure the $\bar\nu_e$ flux coming from the Earth to get geophysical information, with possible applications in the interpretation of the geomagnetism.

The KamLAND collaboration has recently reported the first observation of the geoneutrinos (Araki *et al.*, 2005a). The events are identified by the time and distance coincidence between the prompt e^+ and the delayed (200 μs) neutron capture produced by $\bar\nu_e + p \to n + e^+$ and emiting a 2.2 MeV gamma. The energy window to search for the geoneutrino events is $[1.7, 3.4]$ MeV: the lower bound corresponds to the reaction threshold while the upper bound is constrained by nuclear reactor induced background events.

The measured rate in the 1 kT liquid scintillator detector located at Kamioka (Japan) is 25^{+19}_{-18} for a total background of 127 ± 13 events.

The background is composed by 2/3 of $\bar\nu_e$ from the nuclear reactors in Japan and Korea[3] and 1/3 of events coming from neutrons of 7.3 MeV produced in ^{13}C$(\alpha,n)^{16}$O reactions and captured as in the inverse beta decay reaction. The α particles come from the ^{210}Po decays, a

[3] These events have been used by KamLAND to confirm and measure precisely the Solar driven neutrino oscillation parameters XI.

^{222}Rn daughter which is of natural radioactivity origin. The measured geoneutrino events can be converted in a rate of $5.1^{+3.9}_{-3.6}$ 10^{-31} $\bar{\nu}_e$ per target proton per year corresponding to a mean flux of 5.7 10^6cm^{-2} s^{-1}, or this can be transformed into a 99% CL upper bound of 1.45 10^{-30} $\bar{\nu}_e$ per target proton per year (1.62 10^7cm^{-2} s^{-1} and 60 TW for the radiogenic power).

In MEMPHYS, one expects 10 times more geoneutrino events but this would imply to decrease the trigger threshold to 2 MeV which seems very challenging with respect to the present SuperKamiokande threshold set to 4.6 MeV due to high level of raw trigger rate 120 Hz and increasing by a factor 10 each times the trigger is lowered by 1 MeV (Fukuda *et al.*, 2003). This trigger rate is driven by a number of factors as dark current of the PMT, γs from the rock surrounding the detector, radioactive decay in the PMT glass itself and Radon contamination in the water.

In LENA at the underground laboratory at CUPP a geoneutrino rate of roughly 1000/y (Hochmuth *et al.*, 2005) from the dominant $\bar{\nu}_e + p \rightarrow e^+ + n$ inverse beta-decay reaction is expected. The delayed coincidence measurement of the positron and the 2.2 MeV gamma event, following neutron capture on protons in the scintillator provides a very efficient tool to reject background events. The threshold energy of 1.8 MeV allows the measurement of geoneutrinos from the Uranium and Thorium series, but not from ^{40}K. A reactor background rate of about 240 events per year for LENA at CUPP in the relevant energy window from 1.8 MeV to 3.2 MeV has been calculated.

This background can be subtracted statistically using the information on the entire reactor neutrino spectrum up to $\simeq$ 8 MeV. As it was shown in KamLAND a serious background source may come from radio impurities. There the correlated background from the isotope ^{210}Po is dominating. However, with an enhanced radiopurity of the scintillator, the background can be significantly reduced. Taking the radio purity levels of the CTF detector, where a ^{210}Po activity of 35 ± 12/m^{3}d in PXE has been observed, this background would be reduced by a factor of about 150 compared to KamLAND and would account to less than 10 events per year in the LENA detector. An additional background that imitates the geoneutrino signal is due to ^{9}Li, which is produced by cosmic muons in spallation reactions with ^{12}C and decays in a β-neutron cascade. Only a small part of the ^{9}Li decays falls into the energy window which is relevant for geoneutrinos. KamLAND estimates this background to be 0.30 ± 0.05 (Araki *et al.*, 2005a). At CUPP the muon reaction rate would be reduced by a factor $\simeq$ 10 due to better shielding and this background rate should be at the negligible level of $\simeq$ 1 event per year in LENA.

From this considerations we follow that LENA would be a very capable detector for measuring geoneutrinos. Different Earth's models could be tested with great significance. The sensitivity of LENA for probing the unorthodox idea of a geo-reactor in the Earth's core was

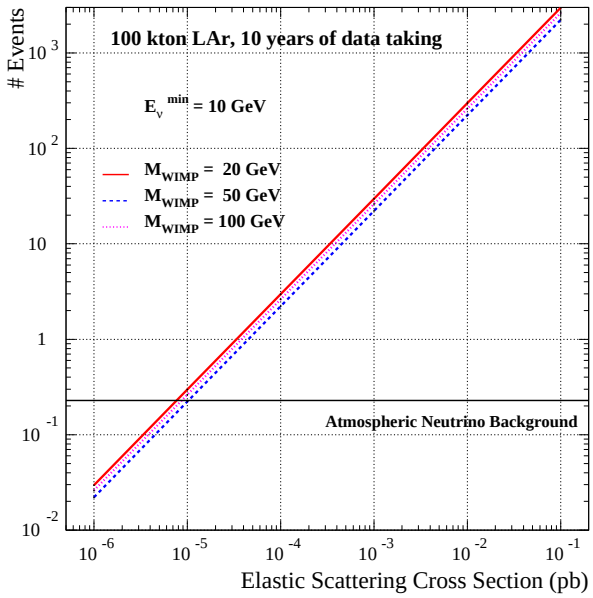

FIG. 14 Expected number of signal and background events as a function of the WIMP elastic scattering production cross section in the Sun, with a cut of 10 GeV on the minimum neutrino energy.

estimated too. At the CUPP underground laboratory in Pyhäsalmi the neutrino background with energies up to $\simeq$ 8 MeV due to nuclear power plants was calculated to be around 2200 events per year. At CUPP a 2 TW georeactor in the Earth's core would contribute 420 events per year and could be identified at a statistical level of better than 3σ after only one year of measurement.

Finally, in GLACIER the $\bar{\nu}_e + {}^{40}Ar \rightarrow e^+ + {}^{40}Cl^*$ has a threshold of 7.5 MeV which is too high for geoneutrino detection.

IX. INDIRECT SEARCH FOR DARK MATTER

WIMPs that constitute the halo of the Milky Way can occasionally interact with massive objects, such as stars or planets. When they scatter off of such an object, they can potentially lose enough energy that they become gravitationally bound and eventually will settle in the center of the celestial body. In particular, WIMPs can be captured by and accumulate in the core of the Sun.

We have assessed, in a model-independent way, the capabilities that GLACIER offers for identifying neutrino signatures coming from the products of WIMP annihilations in the core of the Sun (Bueno *et al.*, 2005). Signal events will consist of energetic electron (anti)neutrinos coming from the decay of τ leptons and b quarks produced in WIMP annihilation in the core of the Sun. Background contamination from atmospheric neutrinos is expected to be low. We do not consider the possibil-

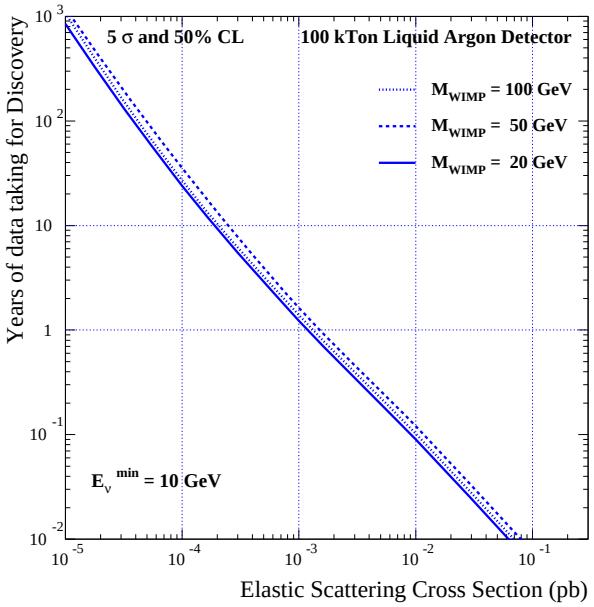

FIG. 15 Minimum number of years required to claim a discovery WIMP signal from the Sun in a 100 kton LAr detector as function of $\sigma_{\rm elastic}$ for three values of the WIMP mass.

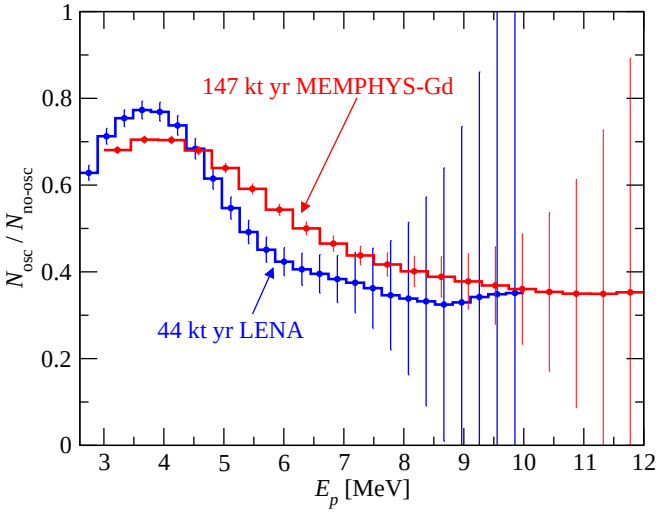

FIG. 16 The ratio of the event spectra in positron energy in the case of oscillations with $\Delta m^2_{21} = 7.9 \times 10^{-5}$ eV^2 and $\sin^2\theta_{12} = 0.30$ and in the absence of oscillations, determined using one year data of MEMPHYS-Gd and LENA located at Frejus. The error bars correspond to 1σ statistical error.

ity of observing neutrinos from WIMPs accumulated in the Earth. Given the smaller mass of the Earth and the fact that only scalar interactions contribute, the capture rates for our planet are not enough to produce, in our experimental set-up, a statistically significant signal.

Our search method takes advantage of the excellent angular reconstruction and superb electron identification capabilities GLACIER offers to look for an excess of energetic electron (anti)neutrinos pointing in the direction of the Sun. The expected signal and background event rates have been evaluated, in a model independent way, as a function of the WIMP's elastic scatter cross section for a range of masses up to 100 GeV.

The detector discovery potential, i.e. the number of years needed to claim a WIMP signal has been discovered, is shown in Figs. 14 and 15. With the assumed set-up and thanks to the low background environment offered by the LAr TPC, a clear WIMP signal would be detected provided the elastic scattering cross section in the Sun is above $\sim 10^{-4}$ pb.

X. NEUTRINOS FROM REACTORS

The KamLAND 1 kT liquid scintillator detector located at Kamioka in Japan had measured the flux of 53 power reactors corresponding to 701 Joule/cm^2 (Araki *et al.*, 2005b). An event rate of 365.2±23.7 above 2.6 MeV for an exposure of 766 ton.y from this nuclear power reactors was expected. The observed rate was 258 events with a total of background of 17.8±7.3. The clear deficit interpreted in terms of neutrino oscillation enables a measurement of θ_{12}, the neutrino 1-2 family mixing angle ($\sin^2\theta_{12} = 0.31^{+0.02}_{-0.03}$) as well as the mass squared difference $\Delta m^2_{12} = 7.9 \pm 0.3\ 10^{-5}$eV^2 (error quoted at 1 σ).

Future precision measurements are currently been investigated. Running KamLAND for 2-3 more years would gain 30% (4%) reduction in the spread of Δm^2_{12} (θ_{12}). Although it has been shown in sections V and VIII that $\bar{\nu}_e$ originated from nuclear reactors can be a serious background for diffuse supernova neutrino and geoneutrino detections, the Fréjus site can take benefit of the nuclear reactors located in the Rhône valley to measure Δm^2_{21} and $\sin^2\theta_{12}$.

In fact approximately 67% of the total reactor $\bar{\nu}_e$ flux at Fréjus originates from four nuclear power plants in the Rhone valley, located at distances between 115 km and 160 km. The indicated baselines are particularly suitable for the study of the $\bar{\nu}_e$ oscillations driven by Δm^2_{21}—they are similar to those exploited in the KamLAND experiment. The authors of (Petcov and Schwetz, 2006) have investigated the possibility to use one module of MEMPHYS (147 kt fiducial mass) doped with Gadolinium (MEMPHYS-Gd) or the LENA detector, updating the previous work of (Choubey and Petcov, 2004). Above 3 MeV (2.6 MeV) the event rate is 59,980 (16,670) events/yr for MEMPHYS-Gd (LENA), which is 2 orders of magnitude larger than the KamLAND event rate.

To test the sensitivity of the experiments the prompt energy spectrum is divided into 20 bins between 3 MeV and 12 MeV for MEMPHYS-Gd and SK-Gd, and into 25 bins between 2.6 MeV and 10 MeV for LENA (Fig. 16).

A χ^2 analysis taking into account the statistical and systematical errors shows that each of the two detectors, MEMPHYS-Gd and LENA, if placed at Fréjus, would allow a very precise determination of the solar neutrino

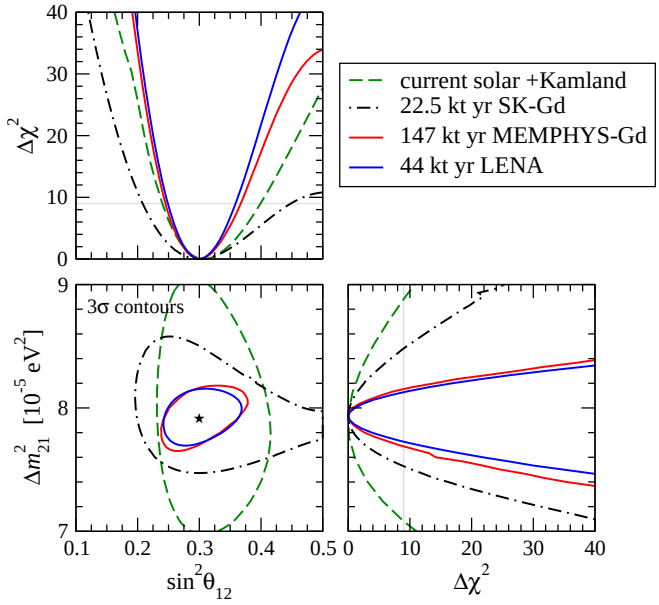

FIG. 17 The accuracy of the determination of Δm^2_{21} and $\sin^2\theta_{12}$, which can be obtained using one year of data from MEMPHYS-Gd and LENA at Frejus, and from SK-Gd at Kamioka, compared to the current precision from solar neutrino and KamLAND data. We show the allowed regions at 3σ (2 d.o.f.) in the $\Delta m^2_{21} - \sin^2\theta_{12}$ plane, as well as the projections of the χ^2 for each parameter.

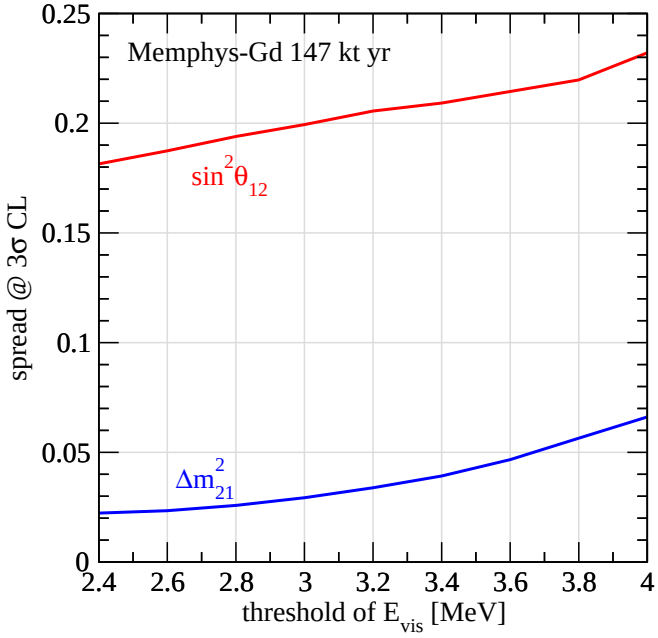

FIG. 18 The accuracy of the determination of Δm^2_{21} and $\sin^2\theta_{12}$, which can be obtained using one year of data from MEMPHYS-Gd as a function of the prompt energy threshold.

oscillation parameters Δm^2_{21} and $\sin^2\theta_{12}$: with one year, the 3σ uncertainties on Δm^2_{21} and $\sin^2\theta_{12}$ can be reduced respectively to less than 3% and to approximately 20% (see also Fig. 17). In comparison, the Gadolinium doped Super-Kamiokande detector (SK-Gd) that might be envisaged in a near future can reach a similar precision if the SK/MEMPHYS fiducial mass ratio of 1 to 7 is compensated by a longer SK-Gd data taking time. Several years of reactor $\bar{\nu}_e$ data collected by MEMPHYS-Gd or LENA would allow a determination of Δm^2_{21} and $\sin^2\theta_{12}$ with uncertainties of approximately 1% and 10% at 3σ, respectively.

However, some caveat are worth to be mentioned. The prompt energy trigger of 3 MeV requires a very low PMT dark current rate in case of MEMPHYS detector. If the energy threshold is higher then the parameter precision decreases as can be seen on Fig. 18 (Schwetz, 2006). The systematic uncertainties are also an important factor in the experiments under consideration, especially the determination of the mixing angle (eg. the energy scale and the overall normalization). Anyhow the accuracies on the solar oscillation parameters, which can be obtained in the high statistics experiments considered here are comparable to those that can be reached for the atmospheric neutrino oscillation parameters Δm^2_{31} and $\sin^2\theta_{23}$ in future long-baseline superbeam experiments like T2HK in Japan or SPL from CERN to MEMPHYS. Hence, such reactor measurements would complete the program of the high precision determination of the leading neutrino oscillation parameters.

XI. NEUTRINOS FROM BEAMS

A. Introduction

In this section, we review the physics program offered by the proposed detectors using different accelerator based neutrino beams to push the search for a tiny non-zero θ_{13} or the measurement in case of previous discovery for instance at reactor based experiment such Double-CHOOZ; the search for possible leptonic CP violation ($\delta_{\rm CP}$); the determination of the mass hierarchy (i.e. the sign of Δm^2_{31}) and the θ_{23} octant (i.e. $\theta_{23} > 45°$ or $\theta_{23} < 45°$). We cover the potentiality of Liquid Argon detectors in an upgraded version of the existing CERN to Gran Sasso (CNGS) neutrino beam, and the MEMPHYS detector at the Fréjus site using a possible new CERN proton driver (SPL) to upgrade to 4MW the conventional neutrino beams (so-called Super Beams) and/or a possible new scheme of pure electron (anti)neutrino production by using radioactive ion decays (so-called βB Beam). Note that LENA is considered also as a candidate detector for the latter beam. Finally, as an ultimate tool, one thinks of producing very intense neutrino beams by mean of muon decays (so-called Neutrino Factory) that may be detected with a Liquid Argon detector as large as GLACIER.

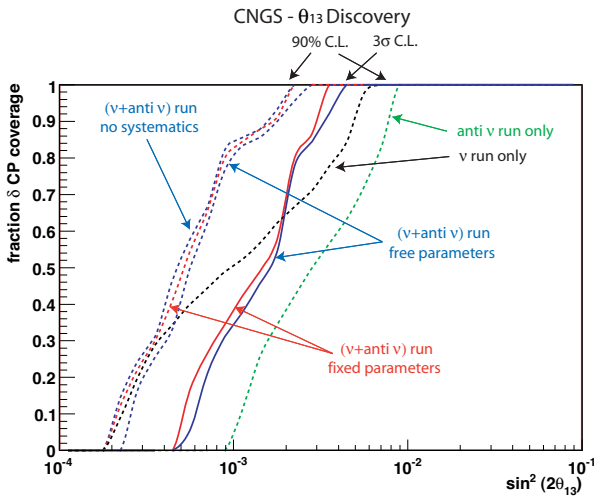

FIG. 19 Sensitivity to discover θ_{13}: the fraction of δ_{CP} coverage as a function of $\sin^2 2\theta_{13}$.

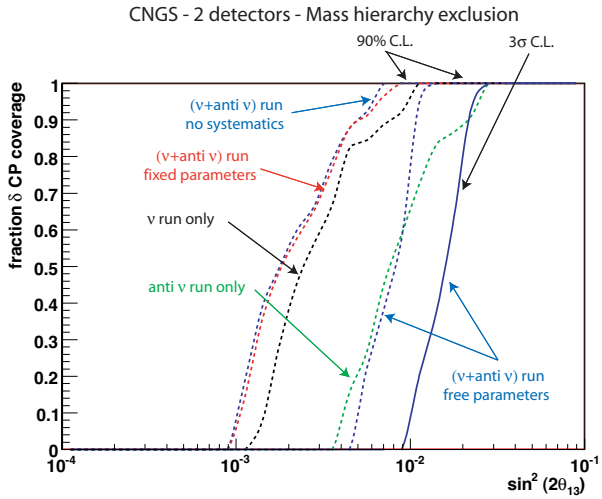

FIG. 20 Mass hierarchy determination for a two detector configuration at baselines of 850 km and 1050 km.

B. CNGS upgraded beam

The determination of the missing U_{e3} element (magnitude and phase) of the PMNS neutrino mixing matrix is possible via the detection of $\nu_\mu \rightarrow \nu_e$ oscillations at a baseline L and energy E given by the atmospheric observations, corresponding to a mass squared difference $E/L \sim \Delta m^2 \simeq 2.5 \times 10^{-3}\ eV^2$. While the current optimization of the CNGS beam provides limited sensitivity to this reaction, we discuss the physics potential of an intensity-upgraded and energy-reoptimized CNGS neutrino beam coupled to an off-axis GLACIER detector (Meregaglia and Rubbia, 2006). This idea is based on the possible upgrade of the CERN PS or on a new machine (PS+) to deliver protons around 50 GeV/c with a power of 200 kW. Post acceleration to SPS energies followed by extraction to the CNGS target region should allow to reach MW power, with neutrino energies peaked around 2 GeV.

To evaluate the physics potential we have assumed five years of running in the neutrino horn polarity plus five additional years in the anti-neutrino mode. We consider a systematic error on the knowledge of the ν_e component of 5%. Given the superb π^0 identification capabilities of GLACIER, the contamination on π^0 is negligible.

An off-axis search for ν_e appearance is performed with the GLACIER detector located at 850 km from CERN. For an off-axis angle of 0.75^o, we observe that θ_{13} can be discovered with 100% probability (full δ_{CP} coverage) for $\sin^2 2\theta_{13} > 0.004$ at 3σ (see Fig. 19).

At this rather modest baseline, the effect of CP-violation and matter effects cannot be disentangled. In fact, the determination of mass hierarchy with at half-coverage (50%) is reached only for $\sin^2 2\theta_{13} > 0.03$ at 3σ. A bigger baseline (1050 km) and a bigger off-axis angle (1.5^o) allows to be sensitive to the first minimum and the second maximum of the oscillation. This is key to resolve the issue of mass hierarchy. With this detector configuration, full coverage for δ_{CP} to determine the mass hierarchy can be reached for $\sin^2 2\theta_{13} > 0.04$ at 3σ. The sensitivity to mass hierarchy determination can be improved by considering two off-axis detectors: one of 30 kton at 850 km and off-axis angle 0.75^o, a second one of 70 kton at 1050 km and 1.5^0 off-axis. Full coverage for δ_{CP} to determine the mass hierarchy can be reached for $\sin^2 2\theta_{13} > 0.02$ at 3σ (see Fig. 20). This two-detector configuration reaches very similar sensitivities to the ones of the T2KK proposal (Ishitsuka *et al.*, 2005).

C. The CERN-SPL Super Beam

The CERN-SPL Super Beam project is a conventional neutrino beam although based on a 4MW SPL (Superconducting Proton Linac) (Gerigk *et al.*, 2006) proton driver impinging a liquid mercury target to generate an intense π^+ (π^-) beam with small contamination of kaon mesons.

The use of a near and far detector will allow for both ν_μ disappearance and $\nu_\mu \rightarrow \nu_e$ appearance studies. The physics potential of the SPL Super Beam with MEMPHYS has been extensively studied (see (Baldini *et al.*, 2006; Campagne *et al.*, 2006; Dornan *et al.*, 2006) for recent studies); however, the beam simulation will need some retuning after HARP results (Catanesi *et al.*, 2001).

After 5 years exposure in ν_μ disappearance mode, a 3σ accuracy of (3-4)% can be acheived on Δm^2_{31}, and an accuracy of 22% (5%) on $\sin^2 \theta_{23}$ if the true value is 0.5 (0.37) that is to say in case of a maximal mixing or a non-maximal mixing (Fig. 21). The use of atmospheric neutrinos (ATM) can alleviate the octant ambiguity in case of non-maximal mixing as it is shown in Fig. 21. Note however, thanks to a higher energy beam ($\sim$ 750 MeV),

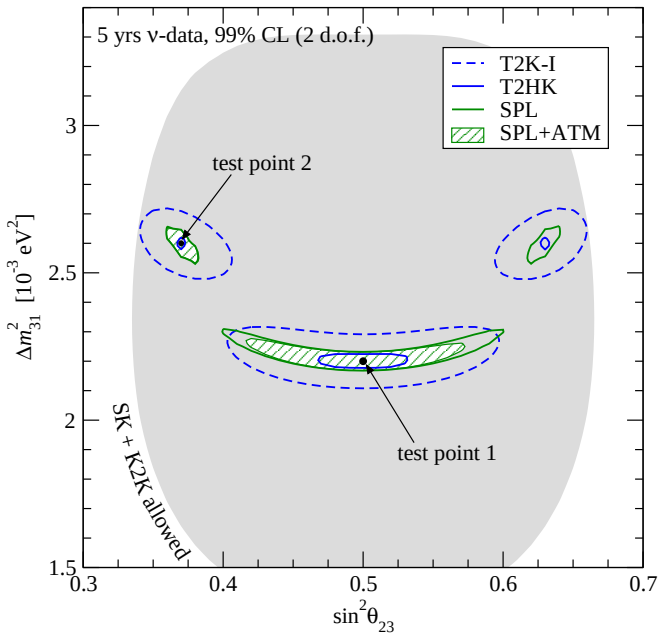

FIG. 21 Allowed regions of Δm^2_{31} and $\sin^2\theta_{23}$ at 99% CL (2 d.o.f.) after 5 yrs of neutrino data taking for SPL, T2K phase I, T2HK, and the combination of SPL with 5 yrs of atmospheric neutrino data in the MEMPHYS detector. For the true parameter values we use $\Delta m^2_{31} = 2.2\,(2.6) \times 10^{-3}$ eV^2 and $\sin^2\theta_{23} = 0.5\,(0.37)$ for the test point 1 (2), and $\theta_{13} = 0$ and the solar parameters as: $\Delta m^2_{21} = 7.9 \times 10^{-5}$ eV^2, $\sin^2\theta_{12} = 0.3$. The shaded region corresponds to the 99% CL region from present SK and K2K data (Maltoni *et al.*, 2004).

the T2HK project[4] can benefit from a much lower dependance on the Fermi motion to obtain a better energy resolution and consequently better results.

In appearance mode (2 years ν_μ plus 8 years $\bar{\nu}_\mu$), a 3σ discovery of non-zero θ_{13}, irrespective of the actual true value of $\delta_{\rm CP}$, is achieved for $\sin^2 2\theta_{13} \gtrsim 4\ 10^{-3}$ ($\theta_{13} \gtrsim 3.6°$) as shown on Fig. 22. For maximal CP violation ($\delta^{\rm true}_{\rm CP} = \pi/2, 3\pi/2$) the same discovery level can be achieved for $\sin^2 2\theta_{13} \gtrsim 8\ 10^{-4}$ ($\theta_{13} \gtrsim 0.8°$). The best sensitivity for testing CP violation (i.e the data cannot be fitted with $\delta_{\rm CP} = 0$ nor $\delta_{\rm CP} = \pi$) is achieved for $\sin^2 2\theta_{13} \approx 10^{-3}$ ($\theta_{13} \approx 0.9°$) as shown on Fig. 23. The maximal sensitivity is achieved for $\sin^2 2\theta_{13} \sim 10^{-2}$ where the CP violation can be established at 3σ for 73% of all the $\delta^{\rm true}_{\rm CP}$.

[4] Here, we make reference to the project where a 4MW proton driver may be build at KEK laboratory to deliver an intense neutrino beam, which send to Kamioka mine is detected by a large Water Čerenkov detector.

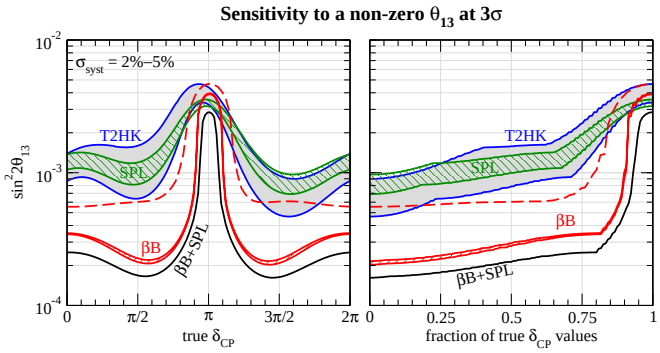

FIG. 22 3σ discovery sensitivity to $\sin^2 2\theta_{13}$ for βB, SPL, and T2HK as a function of the true value of $\delta_{\rm CP}$ (left panel) and as a function of the fraction of all possible values of $\delta_{\rm CP}$ (right panel). The width of the bands corresponds to values for the systematical errors between 2% and 5%. The dashed curve corresponds to the βB sensitivity with the fluxes reduced by a factor 2.

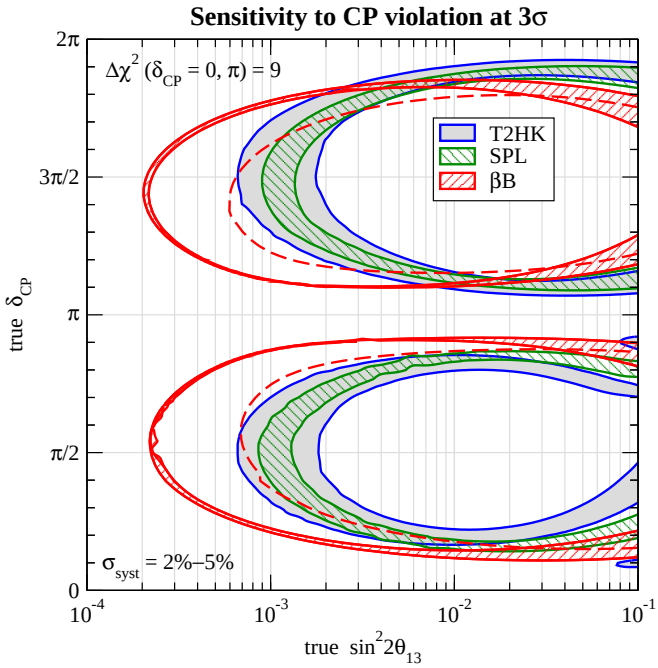

FIG. 23 CPV discovery potential for βB, SPL, and T2HK: For parameter values inside the ellipse-shaped curves CP conserving values of $\delta_{\rm CP}$ can be excluded at 3σ ($\Delta\chi^2 > 9$). The width of the bands corresponds to values for the systematical errors from 2% to 5%. The dashed curve is described in Fig. 22.

D. The CERN-βB baseline scenario

Although quite powerful, the SPL Super Beam is a conventional neutrino beam with known limitations due to 1) a lower production rate of anti-neutrinos compared to neutrinos which in addition to a smaller charged current cross-section impose to run 4 times longer in anti-neutrino modes; 2) the difficulty to setup a accurate beam simulation which implies to the design of a non-

trivial near detector setup (cf. K2K, MINOS, T2K) to master the background level. Thus, a new type of neutrino beam, the so-called βBis being considered.

The idea is to generate pure, well collimated and intense $\nu_e(\bar{\nu}_e)$ beams by producing, collecting, accelerating radioactive ions. The resulting βB spectra can be easily computed knowing the beta decay spectrum of the parent ion and the Lorentz boost factor γ, and these beams are virtually background free from other flavors. The best ion candidates so far are ^{18}Ne and ^{6}He for $\nu_e$and $\bar{\nu}_e$, respectively.

A baseline study for the βB has been initiated at CERN, and is now going on within the European FP6 design study for EURISOL. The potential of such βB sent to MEMPHYS has been studied in the context of the baseline scenario, using reference fluxes of $5.8{\cdot}10^{18}$ ^{6}He useful decays/year and $2.2{\cdot}10^{18}$ ^{18}Ne decays/year, corresponding to a reasonable estimate by experts in the field of the ultimately achievable fluxes. The optimal values is actually $\gamma = 100$ for both species, and the corresponding performances have been recently reviewed in reference (Baldini *et al.*, 2006; Campagne *et al.*, 2006; Dornan *et al.*, 2006).

On Figs. 22,23 the results of running a βB during 10 years (5 years with neutrinos and 5 years with anti-neutrinos) is shown and prove to be far better compared to a SPL Super beam run, especially for maximal CP violation where a non-zero θ_{13} value can be stated at 3σ for $\sin^2 2\theta_{13} \gtrsim 2\ 10^{-4}$ ($\theta_{13} \gtrsim 0.4°$). Moreover, it is noticeable that the βB is less affected by systematic errors on the background compared to the SPL Super beam and T2HK.

Before combining the two possible CERN beams, let us consider LENA as potential detector. LENA (with a fiducial volume of ~ 45 kt) can as well be used as detector for a low-energy βB oscillation experiment. In the energy range $0.2-1.2$ GeV, the performed simulations show that muon events are separable from electron events due to their different track lengths in the detector and due to the electron emitted in the muon decay.

For high energies, muons travel longer than electrons as electrons undergo scattering and bremsstrahlung. This results in different distributions of the number of photons and the timing pattern, which can be used to distinguish between the two classes of events. For low energies, muons can be recognized by observing the electron of its succeeding decay after a mean time of 2.2 μs. Using both criteria, an efficiency of ~ 90 % for muon appearance has been calculated with acceptance of 1 % electron background.

The advantage of using a liquid scintillator detector for such an experiment is the good energy reconstruction of the neutrino beam. However, neutrinos of these energies can produce delta resonances which subsequently decay into a nucleon and a pion. In Water Čerenkov detectors, pions with energies under the Čerenkov threshold contribute to the uncertainty of the neutrino energy. In LENA these particles can be detected. The effect of pion production and similar reactions is currently under investigation in order to estimate the actual energy resolution.

To conclude this section, let us mention a very recent development of the βB concept: first, authors of reference (Rubbia *et al.*, 2006) are considering a very promising alternative for the production of ions, and secondly, the possibility to have monochromatic, single flavor neutrino beams by using ions decaying through the electron capture process (Bernabeu *et al.*, 2005; Sato, 2005). Such beams would in particular be perfect to precisely measure neutrino cross sections in a near detector with the possibility of an energy scan by varying the γ value of the ions.

E. combining SPL Beam and βB with MEMPHYS at Fréjus

Since a βB uses only a small fraction of the protons available from the SPL, Super and Beta beams can be run at the same time. The combination of Super and β beams offers advantages, from the experimental point of view, since the same parameters θ_{13} and δ_{CP} may be measured in many different ways, using 2 pairs of CP related channels, 2 pairs of T related channels, and 2 pairs of CPT related channels which should all give coherent results. In this way the estimates of the systematic errors, different for each beam, will be experimentally cross-checked. And, needless to say, the unoscillated data for a given beam will give a large sample of events corresponding to the small searched-for signal with the other beam, adding more handles on the understanding of the detector response.

Their combination after 10 years leads to minor improvements on the sensitivity on θ_{13} and $\delta_{\rm CP}$ compare to the βB alone results as shown on Fig. 22. But, the important point considering the combination of the βB and the Super Beam is looking at neutrino modes only: ν_μ for SPL and ν_e for βB. If CPT symmetry is assumed, all the information can be obtained as $P_{\bar{\nu}_e\to\bar{\nu}_\mu} = P_{\nu_\mu\to\nu_e}$ and $P_{\bar{\nu}_\mu\to\bar{\nu}_e} = P_{\nu_e\to\nu_\mu}$. We illustrate this synergy in Fig. 24. In this scenario, time consuming anti-neutrino running can be avoided keeping the same physics discovery potential.

One can also combine SPL, βB and the atmospheric neutrinos (ATM) to alleviate the parameter degeneracies which lead to disconnected regions on the multi-dimensional space of oscillation parameters[5]. Atmospheric neutrinos, mainly multi-GeV e-like events, are sensitive to the neutrino mass hierarchy if θ_{13} is sufficiently large due to Earth matter effects, whilst sub-GeV e-like events provide sensitivity to the octant of θ_{23} due to oscillations with Δm^2_{21}.

[5] See reference (Burguet-Castell *et al.*, 2001; Fogli and Lisi, 1996; Minakata and Nunokawa, 2001) for the definitions of *intrinsic*, *hierarchy*, and *octant* degeneracies

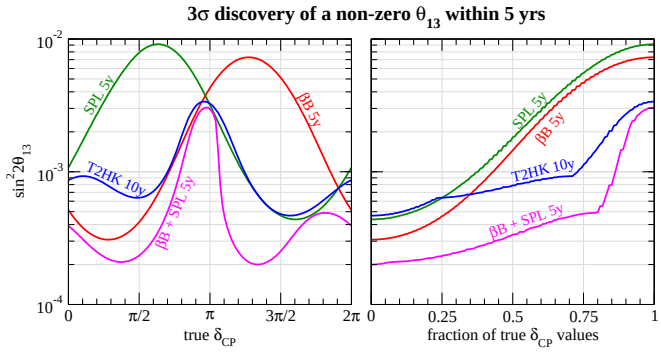

FIG. 24 Discovery potential of a finite value of $\sin^2 2\theta_{13}$ at 3σ ($\Delta\chi^2 > 9$) for 5 yrs neutrino data from βB, SPL, and the combination of βB + SPL compared to 10 yrs data from T2HK (2 yrs neutrinos + 8 yrs antineutrinos).

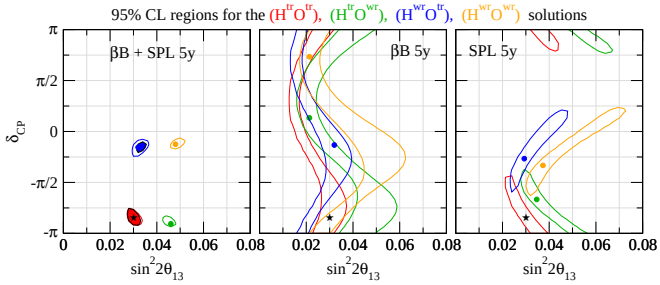

FIG. 25 Allowed regions in $\sin^2 2\theta_{13}$ and δ_{CP} for 5 years data (neutrinos only) from βB, SPL, and the combination. $H^{tr/wr}(O^{tr/wr})$ refers to solutions with the true/wrong mass hierarchy (octant of θ_{23}). For the colored regions in the left panel also 5 years of atmospheric data are included; the solution with the wrong hierarchy has $\Delta\chi^2 = 3.3$. The true parameter values are $\delta_{CP} = -0.85\pi$, $\sin^2 2\theta_{13} = 0.03$, $\sin^2\theta_{23} = 0.6$. For the βB only analysis (middle panel) an external accuracy of 2% (3%) for $|\Delta m^2_{31}|$ (θ_{23}) has been assumed, whereas for the left and right panel the default value of 10% has been used.

The result of running during 5 years on neutrino mode for SPL and βB, adding further the ATM data, is shown on Fig. 25 (Campagne *et al.*, 2006). One can appreciate that practically all the degeneracies can be eliminated as only the solution with the wrong sign survives with a $\Delta\chi^2 = 3.3$. This last degeneracy can be completely eliminated using neutrino mode combined with anti-neutrino mode and ATM data (Campagne *et al.*, 2006), however the example shown is a favorable case with $\sin^2\theta_{23} = 0.6$, and in general for $\sin^2\theta_{23} < 0.5$ the impact of the atmospheric data is weaker.

So, as a generic case, for the CERN-MEMPHYS project, one is left with the four intrinsic degeneracies. However, the important observation of Fig. 25 is that degeneracies have only a very small impact on the CP violation discovery, in the sense that if the true solution is CP violating also the fake solutions are located at CP violating values of $\delta_{\rm CP}$. Therefore, thanks to the relatively short baseline without matter effect, even if degeneracies affect the precise determination of θ_{13} and $\delta_{\rm CP}$, they have only a small impact on the CP violation discovery potential. Furthermore, one would quote explicitly the four possible set of parameters with their respective confidential level. It is also clear from the figure that the sign(Δm^2_{31}) degeneracy has practically no effect on the θ_{13} measurement, whereas the octant degeneracy has very little impact on the determination of $\delta_{\rm CP}$. Some other features of the ATM data are presented in Sec. VII.

F. Neutrino Factory LAr detector

In order to fully address the oscillation processes at a neutrino factory, a detector should be capable of identifying and measuring all three charged lepton flavors produced in charged current interactions *and* of measuring their charges to discriminate the incoming neutrino helicity. The GLACIER concept (in its non-magnetized option) provides a background free identification of electron neutrino charged current and a kinematical selection of tau neutrino charged current interactions. We can assume that charge discrimination is available for muons reaching an external magnetized-Fe spectrometer. Another interesting and extremely challenging possibility would consist on magnetizing the whole liquid argon volume (Badertscher *et al.*, 2005). This set-up allows the clean classification of events into electron, right-sign muon, wrong-sign muon and no-lepton categories. In addition, high granularity permits a clean detection of quasi-elastic events, which by detecting the final state proton, provide a selection of the neutrino electron helicity without the need of an electron charge measurement.

TABLE XI Expected events rates for the GLACIER detector in case no oscillations occur for 10^{20} muon decays. We assume E_μ=30 GeV. N_{tot} is the total number of events and N_{qe} is the number of quasi-elastic events.

Event rates for various baselines							
		L=732 km		L=2900 km		L=7400 km	
		N_{tot}	N_{qe}	N_{tot}	N_{qe}	N_{tot}	N_{qe}
	ν_μ CC	2260000	90400	144000	5760	22700	900
μ^-	ν_μ NC	673000	–	41200	–	6800	–
10^{20} decays	$\overline{\nu}_e$ CC	871000	34800	55300	2200	8750	350
	$\overline{\nu}_e$ NC	302000	–	19900	–	3000	–
	$\overline{\nu}_\mu$ CC	1010000	40400	63800	2550	10000	400
μ^+	$\overline{\nu}_\mu$ NC	353000	–	22400	–	3500	–
10^{20} decays	ν_e CC	1970000	78800	129000	5160	19800	800
	ν_e NC	579000	–	36700	–	5800	–

Table XI summarizes the expected rates for GLACIER and 10^{20} muon decays at a neutrino factory with stored muons having an energy of 30 GeV (Bueno *et al.*, 2000). N_{tot} is the total number of events and N_{qe} is the number of quasi-elastic events.

Figure 26 shows the expected sensitivity in the measurement of θ_{13} for a baseline of 7400 km. The maximal

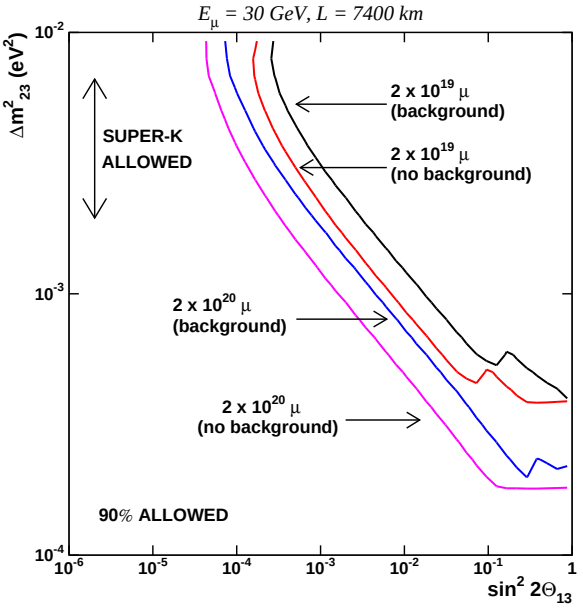

FIG. 26 GLACIER sensitivity for θ_{13}.

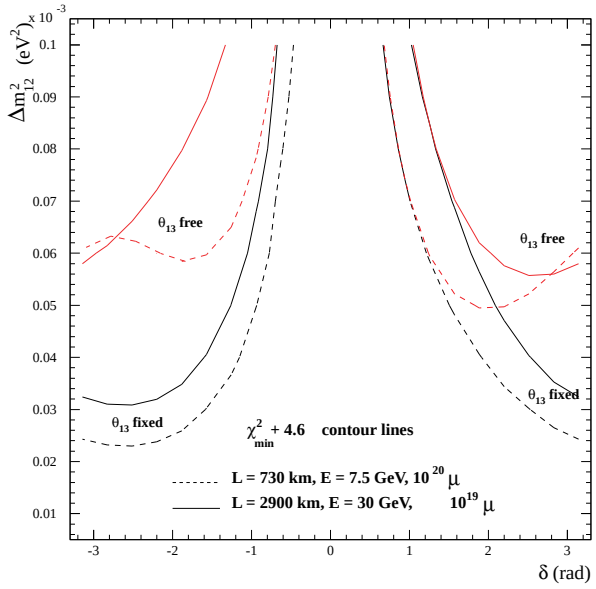

FIG. 27 GLACIER 90% C.L. sensitivity on the CP-phase δ_{CP} as a function of Δm^2_{21} for the two considered baselines. The reference oscillation parameters are $\Delta m^2_{32} = 3 \times 10^{-3}$ eV^2, $\sin^2\theta_{23} = 0.5$, $\sin^2\theta_{12} = 0.5$, $\sin^2 2\theta_{13} = 0.05$ and $\delta_{CP} = 0$. The lower curves are made fixing all parameters to the reference values while for the upper curves θ_{13} is free.

sensitivity to θ_{13} is achieved for very small background levels, since we are looking in this case for small signals; most of the information is coming from the clean wrong-sign muon class and from quasi-elastic events. On the other hand, if its value is not too small, for a measurement of θ_{13}, the signal/background ratio could be not so crucial, and also the other event classes can contribute to this measurement.

A ν-Factory should have among its aims the over constraining of the oscillation pattern, in order to look for unexpected new physics effects. This can be achieved in global fits of the parameters, where the unitarity of the mixing matrix is not strictly assumed. Using a detector able to identify the τ lepton production via kinematic means, it is possible to verify the unitarity in $\nu_\mu \to \nu_\tau$ and $\nu_e \to \nu_\tau$ transitions.

The study of CP violation in the lepton system probably is the most ambitious goal of an experiment at a neutrino factory. Matter effect can mimic CP violation; however, a multi parameter fit at the right baseline can allow a simultaneous determination of matter and CP-violating parameters. To detect CP violation effects, the most favorable choice of neutrino energy E_ν and baseline L is in the region of the "first maximum", given by $(L/E_\nu)^{max} \simeq 500$ km/GeV for $|\Delta m^2_{32}| = 2.5 \times 10^{-3}$ eV^2 (Bueno *et al.*, 2002). To study oscillations in this region, one has to require that the energy of the "first-maximum" be smaller than the MSW resonance energy: $2\sqrt{2} G_F n_e E_\nu^{max} \lesssim \Delta m^2_{32} \cos 2\theta_{13}$. This fixes a limit on the baseline $L_{max} \approx$5000 km beyond which matter effects spoil the sensitivity.

As an example, Fig. 27 shows the sensitivity on the CP violating phase δ_{CP} for two concrete cases. We have classified the events in the five categories previously mentioned, assuming an electron charge confusion of 0.1%. We have computed the exclusion regions in the $\Delta m^2_{12} - \delta_{CP}$ plane fitting the visible energy distributions, provided that the electron detection efficiency is $\sim 20\%$. The excluded regions extend up to values of $|\delta_{CP}|$ close to π, even when θ_{13} is left free.

XII. SUMMARY

The three proposed detectors (MEMPHYS, LENA, GLACIER) based on completely different detection techniques (Water Čerenkov, Liquid Scintillator, Liquid Argon) share to a large extent a very rich physics program and in some cases their detection specificities are complementary. A brief summary of the scientific case is presented both for non-accelerator based topics and the accelerator neutrino oscillation topic on tables XII and XIII, respectively.

Acknowledgments

References

Abdurashitov, D. N., *et al.*, 1994, Phys. Lett. **B328**, 234.

TABLE XII Brief summary of the physics potential of the proposed detectors for non-accelerator based topics. The (*) stands for the case where one MEMPHYS shaft is filled with Gadolinium.

Topics	**GLACIER** (100 kt)	**LENA** (50 kt)	**MEMPHYS** (440 kt)
Proton decay			
$e^+\pi^0$	0.5×10^{35}	-	1.0×10^{35}
$\bar{\nu}K^+$	1.1×10^{35}	0.4×10^{35}	0.2×10^{35}
SN ν (10 kpc)			
CC	2.5 $10^4(\nu_e)$	9.0 $10^3(\bar{\nu}_e)$	2.0 $10^5(\bar{\nu}_e)$
NC	3.0 10^4	3.0 10^3	-
ES	1.0 $10^3(e)$	7.0 $10^3(p)$	1.0 $10^3(e)$
DSN ν (5 yrs Sig./Bkgd)	40-60/30	9-110/7	43-109/47 (*)
Solar ν (1 yr Sig.)	4.5 10^4/1.6 10^5 (^{8}B ES/Abs)	2.0 10^6/7.7 10^4/1.6 10^4/360 (^{7}Be/*pep*/^{8}B ES/^{8}B CC)	1.1 10^5 (^{8}B ES)
Atmospheric ν (1 yr Sig.)	1.1 10^4	TBD	4.0 10^4 (1-ring only)
Geo ν (1 yr Sig.)	below threshold	≈ 1000	need 2 MeV threshold
Reactor ν (1 yr Sig.)	-	1.7 10^4	6.0 10^4 (*)
Dark Matter 10 yrs Sig.	3 events ($\sigma_{ES} = 10^{-4}$,$M > 20$ GeV)	TBD	TBD

TABLE XIII Brief summary of the physics potential of the proposed detectors for accelerator oscillation topic. To be completed

Detector	Beam type	Running time	Potentialities
MEMPHYS	CERN-SPL (disapp.)	5 yrs	$\delta\Delta m^2_{31} = (3-4)\%$ and $\delta \sin^2\theta_{23} = (5-22)\%$
	CERN-βB ($\theta_{13} \neq 0$)	10 yrs	$\sin^2 2\theta^{3\sigma}_{13} \approx 4\ 10^{-3}(2\ 10^{-4})$
	SPL+βB ($\theta_{13} \neq 0$)	5 yrs	$\sin^2 2\theta^{3\sigma}_{13} \approx 3\ 10^{-3}(2\ 10^{-4})$
	CERN-βB (CPV)	10 yrs	$\sin^2 2\theta^{3\sigma}_{13} \approx 2\ 10^{-4}(\delta_{CP} = \frac{\pi}{2}, \frac{3\pi}{2})$
	SPL-βB (CPV)	5 yrs	$\sin^2 2\theta^{3\sigma}_{13} \approx 4\ 10^{-4}(\delta_{CP} = \frac{\pi}{2}, \frac{3\pi}{2})$
	SPL+βB+ATM	10 yrs	2σ mass hier. for $\sin^2 2\theta_{13} \approx 0.02$ + degeneracy reduction
GLACIER			

Aglietta, M., *et al.*, 1987, Europhys. Lett. **3**, 1321.
Aglietta, M., *et al.* (The NUSEX), 1989, Europhys. Lett. **8**, 611.
Agostinelli, S., *et al.* (GEANT4), 2003, Nucl. Instrum. Meth. **A506**, 250.
Aharmim, B., *et al.* (SNO), 2005, Phys. Rev. **C72**, 055502.
Ahn, M. H., *et al.* (K2K), 2006, eprint hep-ex/0606032.
Alekseev, E. N., L. N. Alekseeva, I. V. Krivosheina, and V. I. Volchenko, 1988, Phys. Lett. **B205**, 209.
Alimonti, G., *et al.*, 1998a, Nucl. Instrum. Meth. **A406**, 411.
Alimonti, G., *et al.* (Borexino), 1998b, Astropart. Phys. **8**, 141.
Allison, W. W. M., *et al.* (Soudan-2), 1999, Phys. Lett. **B449**, 137.
Altmann, M., *et al.* (GNO), 2005, Phys. Lett. **B616**, 174.
Ambrosio, M., *et al.* (MACRO), 2001, Phys. Lett. **B517**, 59.
Amerio, S., *et al.* (ICARUS), 2004, Nucl. Instrum. Meth. **A527**, 329.
Ando, S., 2003, Phys. Lett. **B570**, 11.
Ando, S., 2004, Astrophys. J. **607**, 20.
Ando, S., J. F. Beacom, and H. Yuksel, 2005, Phys. Rev. Lett. **95**, 171101.
Anselmann, P., *et al.* (GALLEX), 1992, Phys. Lett. **B285**, 376.
Antonioli, P., *et al.*, 2004, New J. Phys. **6**, 114.
Araki, T., *et al.*, 2005a, Nature **436**, 499.
Araki, T., *et al.* (KamLAND), 2005b, Phys. Rev. Lett. **94**, 081801.
Arneodo, F., *et al.* (ICARUS), 2001, eprint hep-ex/0103008.
Ashie, Y., *et al.* (Super-Kamiokande), 2005, Phys. Rev. **D71**, 112005.
Aulakh, C. S., B. Bajc, A. Melfo, G. Senjanovic, and F. Vissani, 2004, Phys. Lett. **B588**, 196.
Ayres, D. S., *et al.* (NOvA), 2004, eprint hep-ex/0503053.
Babu, K. S., and R. N. Mohapatra, 1993, Phys. Rev. Lett. **70**, 2845.

Back, H. O., *et al.* (Borexino), 2004, eprint physics/0408032.

Badertscher, A., M. Laffranchi, A. Meregaglia, A. Muller, and A. Rubbia, 2005, Nucl. Instrum. Meth. **A555**, 294.

Bajc, B., P. Fileviez Perez, and G. Senjanovic, 2002a, eprint hep-ph/0210374.

Bajc, B., P. Fileviez Perez, and G. Senjanovic, 2002b, Phys. Rev. **D66**, 075005.

Baldini, A., *et al.* (BENE Steering Group), 2006.

Barger, V., P. Huber, and D. Marfatia, 2005, Phys. Lett. **B617**, 167.

Beacom, J. F., W. M. Farr, and P. Vogel, 2002, Phys. Rev. **D66**, 033001.

Beacom, J. F., and M. R. Vagins, 2004, Phys. Rev. Lett. **93**, 171101.

Becker-Szendy, R., *et al.*, 1992, Phys. Rev. **D46**, 3720.

de Bellefon, A., *et al.*, 2006, eprint hep-ex/0607026.

Bernabeu, J., J. Burguet-Castell, C. Espinoza, and M. Lindroos, 2005, JHEP **12**, 014.

Bionta, R. M., *et al.*, 1987, Phys. Rev. Lett. **58**, 1494.

Birks, J. M., 1964.

Bueno, A., M. Campanelli, S. Navas-Concha, and A. Rubbia, 2002, Nucl. Phys. **B631**, 239.

Bueno, A., M. Campanelli, and A. Rubbia, 2000, Nucl. Phys. **B589**, 577.

Bueno, A., R. Cid, S. Navas-Concha, D. Hooper, and T. J. Weiler, 2005, JCAP **0501**, 001.

Bueno, A., *et al.*, 2007, eprint hep-ph/0701101.

Burguet-Castell, J., M. B. Gavela, J. J. Gomez-Cadenas, P. Hernandez, and O. Mena, 2001, Nucl. Phys. **B608**, 301.

Cadonati, L., F. P. Calaprice, and M. C. Chen, 2002, Astropart. Phys. **16**, 361.

Campagne, J. E., M. Maltoni, M. Mezzetto, and T. Schwetz, 2006, eprint hep-ph/0603172.

Catanesi, M. G., *et al.*, 2001, cERN-SPSC-2001-017.

Choubey, S., and S. T. Petcov, 2004, Phys. Lett. **B594**, 333.

Cocco, A. G., A. Ereditato, G. Fiorillo, G. Mangano, and V. Pettorino, 2004, JCAP **0412**, 002.

Daum, K., *et al.* (Frejus.), 1995, Z. Phys. **C66**, 417.

Davis, J., Raymond, D. S. Harmer, and K. C. Hoffman, 1968, Phys. Rev. Lett. **20**, 1205.

Dighe, A. S., M. T. Keil, and G. G. Raffelt, 2003a, JCAP **0306**, 005.

Dighe, A. S., M. T. Keil, and G. G. Raffelt, 2003b, JCAP **0306**, 006.

Dighe, A. S., and A. Y. Smirnov, 2000, Phys. Rev. **D62**, 033007.

Dornan, P., *et al.* (International Scoping Study), 2006, in preparation .

Dorsner, I., and P. F. Perez, 2005a, Phys. Lett. **B625**, 88.

Dorsner, I., and P. F. Perez, 2005b, Nucl. Phys. **B723**, 53.

Dorsner, I., P. F. Perez, and R. Gonzalez Felipe, 2006, Nucl. Phys. **B747**, 312.

Duan, H., G. M. Fuller, J. Carlson, and Y.-Z. Qian, 2006, Phys. Rev. **D74**, 105014.

Emmanuel-Costa, D., and S. Wiesenfeldt, 2003, Nucl. Phys. **B661**, 62.

Ereditato, A., and A. Rubbia, 2005, Nucl. Phys. Proc. Suppl. **139**, 301.

Fogli, G. L., and E. Lisi, 1996, Phys. Rev. **D54**, 3667.

Fogli, G. L., E. Lisi, A. Mirizzi, and D. Montanino, 2004, Phys. Rev. **D70**, 013001.

Fogli, G. L., E. Lisi, A. Mirizzi, and D. Montanino, 2005, JCAP **0504**, 002.

Fogli, G. L., E. Lisi, D. Montanino, and A. Mirizzi, 2003, Phys. Rev. **D68**, 033005.

Friedmann, T., and E. Witten, 2003, Adv. Theor. Math. Phys. **7**, 577.

Fukuda, Y., *et al.* (Super-Kamiokande), 1998, Phys. Rev. Lett. **81**, 1562.

Fukuda, Y., *et al.*, 2003, Nucl. Instrum. Meth. **A501**, 418.

Fukugita, M., and M. Kawasaki, 2003, Mon. Not. Roy. Astron. Soc. **340**, L7.

Fukuyama, T., A. Ilakovac, T. Kikuchi, S. Meljanac, and N. Okada, 2004, JHEP **09**, 052.

Georgi, H., and S. L. Glashow, 1974, Phys. Rev. Lett. **32**, 438.

Gerigk, F., *et al.*, 2006, cERN-2006-006.

Gil-Botella, I., and A. Rubbia, 2003, JCAP **0310**, 009.

Gil-Botella, I., and A. Rubbia, 2004, JCAP **0408**, 001.

Goh, H. S., R. N. Mohapatra, S. Nasri, and S.-P. Ng, 2004, Phys. Lett. **B587**, 105.

Gonzalez-Garcia, M. C., and M. Maltoni, 2004, Phys. Rev. **D70**, 033010.

Gonzalez-Garcia, M. C., and Y. Nir, 2003, Rev. Mod. Phys. **75**, 345.

Hannestad, S., G. G. Raffelt, G. Sigl, and Y. Y. Y. Wong, 2006, Phys. Rev. **D74**, 105010.

Hirata, K., *et al.* (KAMIOKANDE-II), 1987, Phys. Rev. Lett. **58**, 1490.

Hirata, K. S., *et al.* (KAMIOKANDE-II), 1988a, Phys. Lett. **B205**, 416.

Hirata, K. S., *et al.*, 1988b, Phys. Rev. **D38**, 448.

Hirata, K. S., *et al.* (KAMIOKANDE-II), 1989, Phys. Rev. Lett. **63**, 16.

Hirata, K. S., *et al.* (Kamiokande-II), 1992, Phys. Lett. **B280**, 146.

Hochmuth, K., *et al.*, 2005, Accepted for publication in Astropart. Phys. eprint hep-ph/0509136.

Huber, P., M. Maltoni, and T. Schwetz, 2005, Physical Review D **71**, 053006, URL `doi:10.1103/PhysRevD.71.053006`.

Ianni, A., D. Montanino, and F. L. Villante, 2005, Phys. Lett. **B627**, 38.

Ishitsuka, M., T. Kajita, H. Minakata, and H. Nunokawa, 2005, Phys. Rev. **D72**, 033003.

Itow, Y., *et al.*, 2001, eprint hep-ex/0106019.

Jung, C. K., 2000, AIP Conf. Proc. **533**, 29.

Kachelriess, M., *et al.*, 2005, Phys. Rev. **D71**, 063003.

Keil, M. T., G. G. Raffelt, and H.-T. Janka, 2003, Astrophys. J. **590**, 971.

Kim, C. W., and U. W. Lee, 1998, Phys. Lett. **B444**, 204.

Kobayashi, K., *et al.* (Super-Kamiokande), 2005, Phys. Rev. **D72**, 052007.

Lee, D.-G., R. N. Mohapatra, M. K. Parida, and M. Rani, 1995, Phys. Rev. **D51**, 229.

Lunardini, C., and A. Y. Smirnov, 2001, Nucl. Phys. **B616**, 307.

Lunardini, C., and A. Y. Smirnov, 2003, JCAP **0306**, 009.

Malek, M., *et al.* (Super-Kamiokande), 2003, Phys. Rev. Lett. **90**, 061101.

Maltoni, M., T. Schwetz, M. A. Tortola, and J. W. F. Valle, 2004, New J. Phys. **6**, 122.

Marrodán Undagoitia, T., *et al.*, 2005, Phys. Rev. **D72**, 075014.

Marrodán Undagoitia, T., *et al.*, 2006, Prog. Part. Nucl. Phys. **57**, 283.

Meregaglia, A., and A. Rubbia, 2006, eprint hep-ph/0609106.

Minakata, H., and H. Nunokawa, 2001, JHEP **10**, 001.

Murayama, H., and A. Pierce, 2002, Phys. Rev. **D65**, 055009.

Nakaya, T., 2005, Nucl. Phys. Proc. Suppl. **138**, 376.
Nath, P., and P. F. Perez, 2006, eprint hep-ph/0601023.
Oberauer, L., F. von Feilitzsch, and W. Potzel, 2005, Nucl. Phys. Proc. Suppl. **138**, 108.
Odrzywolek, A., M. Misiaszek, and M. Kutschera, 2004, Astropart. Phys. **21**, 303.
Peres, O. L. G., and A. Y. Smirnov, 1999, Phys. Lett. **B456**, 204.
Petcov, S. T., and T. Schwetz, 2006, eprint hep-ph/0607155.
Rubbia, A., 2004a, eprint hep-ph/0402110.
Rubbia, A., 2004b, eprint hep-ph/0407297.
Rubbia, C., A. Ferrari, Y. Kadi, and V. Vlachoudis, 2006, eprint hep-ph/0602032.
Sato, J., 2005, Phys. Rev. Lett. **95**, 131804.
Schirato, R. C., G. M. Fuller, . U. . LANL), UCSD, and LANL), 2002, eprint astro-ph/0205390.
Schwetz, T., 2006.
Smy, M. B. (Super-Kamiokande), 2003, Nucl. Phys. Proc. Suppl. **118**, 25.
Tagg, N. (MINOS), 2006, ECONF **C060409**, 019.
Thompson, T. A., A. Burrows, and P. A. Pinto, 2003, Astrophys. J. **592**, 434.
Tomas, R., D. Semikoz, G. G. Raffelt, M. Kachelriess, and A. S. Dighe, 2003, Phys. Rev. **D68**, 093013.
Tomas, R., *et al.*, 2004, JCAP **0409**, 015.
Totani, T., K. Sato, H. E. Dalhed, and J. R. Wilson, 1998, Astrophys. J. **496**, 216.
Wurm, M., *et al.*, 2006, Submitted for publication in Phys. Rev. D .
Yuksel, H., S. Ando, and J. F. Beacom, 2006, Phys. Rev. **C74**, 015803.